Commun. Comput. Phys.
doi: 10.4208/cicp.OA-2016-0135

Vol. **21**, No. 4, pp. 1173-1206
April 2017

Second-Order Two-Scale Computational Method for Nonlinear Dynamic Thermo-Mechanical Problems of Composites with Cylindrical Periodicity

Hao Dong[1], Junzhi Cui[2,*], Yufeng Nie[1] and Zihao Yang[1]

[1] *Department of Applied Mathematics, School of Science, Northwestern Polytechnical University, Xi'an 710129, P.R. China.*
[2] *LSEC, ICMSEC, Academy of Mathematics and Systems Science, Chinese Academy of Sciences, Beijing 100190, P.R. China.*

Received 16 August 2016; Accepted (in revised version) 5 September 2016

Abstract. In this paper, a novel second-order two-scale (SOTS) computational method is developed for nonlinear dynamic thermo-mechanical problems of composites with cylindrical periodicity. The non-linearities of these multi-scale problems were caused by the temperature-dependent properties of the composites. Firstly, the formal SOTS solutions for these problems are constructed by the multiscale asymptotic analysis. Then we theoretically explain the importance of the SOTS solutions by the error analysis in the pointwise sense. In addition, a SOTS numerical algorithm is proposed in detail to effectively solve these problems. Finally, some numerical examples verify the feasibility and effectiveness of the SOTS numerical algorithm we proposed.

AMS subject classifications: 65M60, 35Q74, 41A60, 74Q10

Key words: Second-order two-scale, nonlinear dynamic thermo-mechanical problems, temperature-dependent properties, cylindrical periodicity.

1 Introduction

In recent years, composite materials have been widely used in engineering applications owing to their excellent physical properties compared to the traditional single component materials, especially in aerospace field. In engineering applications these composites are usually served under complex thermo-mechanical environments. Because of a great application prospect, the thermo-mechanical performances of composite materials have been a research hotspot of scientists and engineers. And it is important to compute the thermo-mechanical responses of the composites in engineering applications.

*Corresponding author. *Email addresses:* donghaonwpu@mail.nwpu.edu.cn (H. Dong), cjz@lsec.cc.ac.cn (J. Cui), yfnie@nwpu.edu.cn (Y. Nie), yangzihao@nwpu.edu.cn (Z. Yang)

 ©2017 Global-Science Press

https://doi.org/10.4208/cicp.OA-2016-0135 Published online by Cambridge University Press

It is known to all that the materials have the temperature-dependent properties when serving in high-temperature circumstances (see [1–3, 26–28, 30]). At this situation, the temperature-dependent properties of the composites should be taken into account in order to perform a more accurate analysis. Up to now, some studies have been performed on dynamic thermo-mechanical problems of composites. Most of these studies focused on one-way thermo-mechanical coupling problems (see [1–4,6–10]), namely only the thermal field affects the mechanical field. Besides, some researchers devoted to the two-way thermo-mechanical coupling problems which are fully coupled hyperbolic and parabolic systems, but their researches were based on the cartesian coordinate system and also didn't consider the temperature-dependent nonlinear effect of material properties [11–15]. In the last few years, some research results for composites with cylindrical geometry structures have appeared [7–10,24,32]. To the best of our knowledge, there is a lack of adequate researches on nonlinear dynamic two-way thermo-mechanical problems of composites with cylindrical periodicity (see Fig. 1).

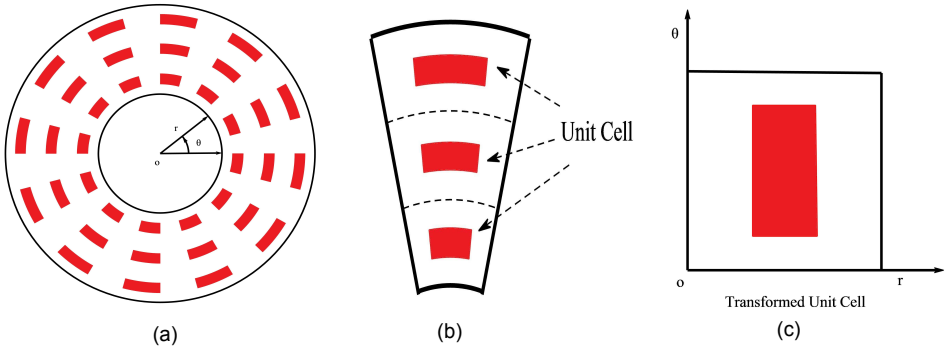


Figure 1: (a) Actual physical area; (b) Actual unit cell; (c) Transformed unit cell Y.

In the past few decades, mathematicians and engineers have developed some multiscale methods to study the multiscale behaviors of the composite materials, such as the asymptotic homogenization method (AHM), heterogeneous multiscale method (HMM), variational multiscale method (VMS), and multiscale finite element method (MsFEM) [29], etc. The AHM is a kind of mathematical method which has a rigorous mathematical foundation and can combine with finite element method very well. So it is widely used to analyze the physical and mechanical behaviors of the composites. We refer the interested readers to [4, 8–10, 29]. However, they only considered the first-order asymptotic expansions. In recent years, Cui et al. introduced the second-order two-scale (SOTS) analysis method [5, 12–14, 16, 17, 33, 34] to accurately predict the physical and mechanical behaviors of composites. By the second-order correctors, the micro-scale fluctuation information of the composites can be captured more precisely.

The aim of this paper is to develop a SOTS computational method for nonlinear dynamic thermo-mechanical problems of composites with cylindrical periodicity. The nonlinearities of these multiscale problems were caused by the temperature-dependent prop-

https://doi.org/10.4208/cicp.OA-2016-0135 Published online by Cambridge University Press

erties of the composites. For non-linearities caused by inelastic constitutive laws in fully coupled thermo-mechanical homogenization, we refer to [31]. Clearly, the direct numerical computation for these multiscale problems needs a tremendous amount of computational resources to capture micro-scale behavior due to large heterogeneities (caused by inclusions or holes) in composite structures. Furthermore, the stability of numerical scheme for this coupled nonlinear system in cylindrical coordinates is also a difficult problem to handle. In order to deal with these difficulties, we develop a SOTS method to overcome numerical difficulties based on asymptotic homogenization method (AHM), finite element method (FEM) and finite difference method (FDM).

This paper is outlined as follows. In Section 2, the detailed construction of the SOTS solutions for nonlinear dynamic thermo-mechanical problems of composites with cylindrical periodicity is given by multiscale asymptotic analysis. Moreover, the error analysis in the pointwise sense of first-order two-scale (FOTS) solutions and SOTS solutions is obtained. By comparing the results of error analysis of FOTS solutions and SOTS solutions in the pointwise sense, we theoretically explain the importance of SOTS solutions in capturing micro-scale information. In Section 3, a SOTS numerical algorithm based on FEM and FDM is presented to effectively solve these multiscale problems. In Section 4, some numerical results are shown to verify the validity of our SOTS algorithm. Finally, some conclusions are given in Section 5.

For convenience, throughout the paper we use the Einstein summation convention on repeated indices. Besides, the notation δ_{ij} is the Kronecker symbol, and if $i=j$, $\delta_{ij}=1$, or $\delta_{ij}=0$. Finally, we do not give the definitions of the associated Sobolev spaces in this paper, and we refer the readers to some classical books (see [18,19]).

2 The governing equations and multiscale asymptotic analysis

Let us consider the following governing equations for nonlinear dynamic thermo-mechanical problems of composites with cylindrical periodicity, whose material parameters all have the temperature-dependent properties:

$$\begin{cases} \rho^\varepsilon(\mathbf{x},T^\varepsilon)\dfrac{\partial^2 u_r^\varepsilon}{\partial t^2}-\Big(\dfrac{\partial\sigma_{rr}^\varepsilon}{\partial r}+\dfrac{1}{r}\dfrac{\partial\sigma_{r\theta}^\varepsilon}{\partial\theta}+\dfrac{\partial\sigma_{rz}^\varepsilon}{\partial z}+\dfrac{\sigma_{rr}^\varepsilon-\sigma_{\theta\theta}^\varepsilon}{r}\Big)=f_r \ \text{ in } \Omega\times(0,T^*),\\ \rho^\varepsilon(\mathbf{x},T^\varepsilon)\dfrac{\partial^2 u_\theta^\varepsilon}{\partial t^2}-\Big(\dfrac{\partial\sigma_{r\theta}^\varepsilon}{\partial r}+\dfrac{1}{r}\dfrac{\partial\sigma_{\theta\theta}^\varepsilon}{\partial\theta}+\dfrac{\partial\sigma_{z\theta}^\varepsilon}{\partial z}+2\dfrac{\sigma_{r\theta}^\varepsilon}{r}\Big)=f_\theta \ \text{ in } \Omega\times(0,T^*),\\ \rho^\varepsilon(\mathbf{x},T^\varepsilon)\dfrac{\partial^2 u_z^\varepsilon}{\partial t^2}-\Big(\dfrac{\partial\sigma_{zr}^\varepsilon}{\partial r}+\dfrac{1}{r}\dfrac{\partial\sigma_{z\theta}^\varepsilon}{\partial\theta}+\dfrac{\partial\sigma_{zz}^\varepsilon}{\partial z}+\dfrac{\sigma_{zr}^\varepsilon}{r}\Big)=f_z \ \text{ in } \Omega\times(0,T^*),\\ \rho^\varepsilon(\mathbf{x},T^\varepsilon)c^\varepsilon(\mathbf{x},T^\varepsilon)\dfrac{\partial T^\varepsilon}{\partial t}+\Big(\dfrac{\partial q_r^\varepsilon}{\partial r}+\dfrac{1}{r}\dfrac{\partial q_\theta^\varepsilon}{\partial\theta}+\dfrac{\partial q_z^\varepsilon}{\partial z}+\dfrac{q_r^\varepsilon}{r}\Big)+\vartheta_{ij}^\varepsilon(\mathbf{x},T^\varepsilon)\dfrac{\partial\varepsilon_{ij}^\varepsilon}{\partial t}=h \ \text{ in } \Omega\times(0,T^*),\\ \mathbf{u}^\varepsilon(\mathbf{x},t)=\widehat{\mathbf{u}}(\mathbf{x},t),\ \ T^\varepsilon(\mathbf{x},t)=\widehat{T}(\mathbf{x},t) \ \text{ on } \partial\Omega\times(0,T^*),\\ \mathbf{u}^\varepsilon(\mathbf{x},0)=\mathbf{u}^0(\mathbf{x}),\ \ \dfrac{\partial\mathbf{u}^\varepsilon(\mathbf{x},t)}{\partial t}\Big|_{t=0}=\mathbf{u}^1(\mathbf{x}),\ \ T^\varepsilon(\mathbf{x},0)=\check{T}(\mathbf{x}) \ \text{ in } \Omega, \end{cases} \tag{2.1}$$

https://doi.org/10.4208/cicp.OA-2016-0135 Published online by Cambridge University Press

where Ω is a bounded convex domain $(0<r<\infty)$ in $\mathbb{R}^3$ with a boundary $\partial\Omega$; The u_r^ε, u_θ^ε, u_z^ε and T^ε in (2.1) are undetermined displacement and temperature fields; $\widehat{\mathbf{u}}(\mathbf{x},t)$, $\widehat{T}(\mathbf{x},t)$, $\mathbf{u}^0(\mathbf{x})$, $\mathbf{u}^1(\mathbf{x})$ and $\check{T}(\mathbf{x})$ are known functions with macro-coordinates $\mathbf{x}=(r,\theta,z)$; ε represents the characteristic periodic unit cell size; ρ^ε and c^ε are the mass density and specific heat; h and f_r, f_θ, f_z are the internal heat source and the body forces; $\widetilde{T}$ is the initial temperature when the composites are stress-free. $\vartheta_{ij}^\varepsilon$ is the nonlinear two-way thermo-mechanical coupled effect tensor; It is stressed that $\vartheta_{ij}^\varepsilon=T^\varepsilon\big[\beta_{ij}^\varepsilon+\frac{\partial\beta_{ij}^\varepsilon}{\partial T^\varepsilon}(T^\varepsilon-\widetilde{T})\big]$ according to the first and second laws of thermodynamics where $\{\beta_{ij}^\varepsilon\}$ is the second order thermal modulus tensor. From theorem 6.1 in [15], we can similarly get the existence and uniqueness of problem (2.1) for fixed ε.

In this paper, for the governing equations (2.1) the strains $\boldsymbol{\varepsilon}^\varepsilon$ are given in terms of the displacements $\mathbf{u}^\varepsilon$ as follows:

$$\begin{aligned}
&\varepsilon_{rr}^\varepsilon=\frac{\partial u_r^\varepsilon}{\partial r},\quad \varepsilon_{\theta\theta}^\varepsilon=\frac{1}{r}\Big(\frac{\partial u_\theta^\varepsilon}{\partial\theta}+u_r^\varepsilon\Big),\qquad \varepsilon_{r\theta}^\varepsilon=\frac{1}{2}\Big(\frac{1}{r}\frac{\partial u_r^\varepsilon}{\partial\theta}+\frac{\partial u_\theta^\varepsilon}{\partial r}-\frac{u_\theta^\varepsilon}{r}\Big),\\
&\varepsilon_{zz}^\varepsilon=\frac{\partial u_z^\varepsilon}{\partial z},\quad \varepsilon_{z\theta}^\varepsilon=\frac{1}{2}\Big(\frac{\partial u_\theta^\varepsilon}{\partial z}+\frac{1}{r}\frac{\partial u_z^\varepsilon}{\partial\theta}\Big),\quad \varepsilon_{rz}^\varepsilon=\frac{1}{2}\Big(\frac{\partial u_z^\varepsilon}{\partial r}+\frac{\partial u_r^\varepsilon}{\partial z}\Big).
\end{aligned}\tag{2.2}$$

If we apply the substitutions: $1\to r$, $2\to\theta$, $3\to z$ and $\psi_1=\frac{\partial}{\partial r}$, $\psi_2=\frac{1}{r}\frac{\partial}{\partial\theta}$, $\psi_3=\frac{\partial}{\partial z}$ to simplify the notations in our paper, the constitutive laws of problem (2.1) are given by

$$\sigma_{ij}^\varepsilon=C_{ijkl}^\varepsilon(\mathbf{x},T^\varepsilon)\varepsilon_{kl}^\varepsilon-\beta_{ij}^\varepsilon(\mathbf{x},T^\varepsilon)(T^\varepsilon-\widetilde{T})\tag{2.3}$$

and

$$q_i^\varepsilon=-k_{ij}^\varepsilon(\mathbf{x},T^\varepsilon)\psi_j(T^\varepsilon),\tag{2.4}$$

where $\{C_{ijkl}^\varepsilon\}$ is the fourth order elastic tensor and $\{k_{ij}^\varepsilon\}$ is the second order thermal conductivity tensor $(i,j,k,l=1,2,3)$.

Now, let us set $\mathbf{y}=\frac{\mathbf{x}}{\varepsilon}=(\frac{r}{\varepsilon},\frac{\theta}{\varepsilon},\frac{z}{\varepsilon})=(\tilde{r},\tilde{\theta},\tilde{z})$ as micro-coordinates of periodic unit cell $Y=(0,1)^3$. With this notation, the material parameters $\rho^\varepsilon(\mathbf{x},T^\varepsilon)$, $c^\varepsilon(\mathbf{x},T^\varepsilon)$, $\vartheta_{ij}^\varepsilon(\mathbf{x},T^\varepsilon)$, $\beta_{ij}^\varepsilon(\mathbf{x},T^\varepsilon)$, $C_{ijkl}^\varepsilon(\mathbf{x},T^\varepsilon)$ and $k_{ij}^\varepsilon(\mathbf{x},T^\varepsilon)$ can be changed into $\rho(\mathbf{y},T^\varepsilon)$, $c(\mathbf{y},T^\varepsilon)$, $\vartheta_{ij}(\mathbf{y},T^\varepsilon)$, $\beta_{ij}(\mathbf{y},T^\varepsilon)$, $C_{ijkl}(\mathbf{y},T^\varepsilon)$ and $k_{ij}(\mathbf{y},T^\varepsilon)$.

Being similar to [13,19,23], some hypotheses of material property parameters in problem (2.1) are listed as follows:

(A) C_{ijkl}^ε, k_{ij}^ε, $\vartheta_{ij}^\varepsilon$ and β_{ij}^ε are symmetric, and there exist two positive constant γ_0 and γ_1 independent of ε such that

$$\begin{aligned}
&C_{ijkl}^\varepsilon=C_{ijlk}^\varepsilon=C_{klij}^\varepsilon,\ \ \gamma_0\eta_{ij}\eta_{ij}\le C_{ijkl}^\varepsilon(\mathbf{x},T^\varepsilon)\eta_{ij}\eta_{kl}\le\gamma_1\eta_{ij}\eta_{ij},\\
&k_{ij}^\varepsilon=k_{ji}^\varepsilon,\ \ \gamma_0|\boldsymbol{\xi}|^2\le k_{ij}^\varepsilon(\mathbf{x},T^\varepsilon)\xi_i\xi_j\le\gamma_1|\boldsymbol{\xi}|^2,\\
&\vartheta_{ij}^\varepsilon=\vartheta_{ji}^\varepsilon,\ \ \gamma_0|\boldsymbol{\xi}|^2\le\vartheta_{ij}^\varepsilon(\mathbf{x},T^\varepsilon)\xi_i\xi_j\le\gamma_1|\boldsymbol{\xi}|^2,\\
&\beta_{ij}^\varepsilon=\beta_{ji}^\varepsilon,\ \ \gamma_0|\boldsymbol{\xi}|^2\le\beta_{ij}^\varepsilon(\mathbf{x},T^\varepsilon)\xi_i\xi_j\le\gamma_1|\boldsymbol{\xi}|^2,
\end{aligned}$$

https://doi.org/10.4208/cicp.OA-2016-0135 Published online by Cambridge University Press

where $\{\eta_{ij}\}$ is an arbitrary symmetric matrix in $R^{3\times3}$, $\boldsymbol{\xi}=(\xi_1,\xi_2,\xi_3)$ an arbitrary vector with real elements in R^3, and $(\mathbf{x},T^\varepsilon)$ is an arbitrary point in $\Omega\times[T_{\min},T_{\max}+C_*]$.

(B) $\begin{cases} \rho^\varepsilon, c^\varepsilon, C^\varepsilon_{ijkl}, k^\varepsilon_{ij}, \vartheta^\varepsilon_{ij} \text{ and } \beta^\varepsilon_{ij} \in L^\infty(\Omega), \\ 0<\rho^0\le\rho^\varepsilon,\ 0<c^0\le c^\varepsilon, \text{ where } \rho^0 \text{ and } c^0 \text{ are constants independent of } \varepsilon, \\ \rho^\varepsilon, c^\varepsilon, C^\varepsilon_{ijkl}, k^\varepsilon_{ij}, \vartheta^\varepsilon_{ij} \text{ and } \beta^\varepsilon_{ij} \text{ are } 1-\text{periodic functions in } \mathbf{y}. \end{cases}$

(C) $f_i\in L^2(\Omega\times(0,T^*))$, $h\in L^2(\Omega\times(0,T^*))$, $\mathbf{u}^0\in(H^1(\Omega))^3$, $\mathbf{u}^1\in(L^2(\Omega))^3$, $\breve{T}\in H^1(\Omega)$, $\widehat{\mathbf{u}}(\mathbf{x},t)\in(L^2(\Omega\times(0,T^*)))^3$, $\widehat{T}(\mathbf{x},t)\in L^2(\Omega\times(0,T^*))$.

In this section, we first give the specific construction process of FOTS solutions and SOTS solutions to problem (2.1). After that, the error analysis in the pointwise sense of FOTS solutions and SOTS solutions is presented which neatly illustrates the extreme necessity of SOTS solutions.

2.1 Second-order two-scale analysis for the governing equations

Enlightened by the works in [9, 10], the operators ψ_i for the macro-scale and $\widetilde{\psi}_i$ for the micro-scale are denoted as follows:

$$\begin{cases} \psi_1=\dfrac{\partial}{\partial r}, & \psi_2=\dfrac{1}{r}\dfrac{\partial}{\partial\theta}, & \psi_3=\dfrac{\partial}{\partial z}, \\ \widetilde{\psi}_1=\dfrac{\partial}{\partial\widetilde{r}}, & \widetilde{\psi}_2=\dfrac{1}{r}\dfrac{\partial}{\partial\widetilde{\theta}}, & \widetilde{\psi}_3=\dfrac{\partial}{\partial\widetilde{z}}. \end{cases} \tag{2.5}$$

Hence, the chain rule of AHM in cylindrical coordinates can be expressed as

$$\psi_i=\psi_i+\varepsilon^{-1}\widetilde{\psi}_i \tag{2.6}$$

which will be extensively used in the sequel.

To the problem (2.1), we suppose that $u^\varepsilon_i(\mathbf{x},t)$ and $T^\varepsilon(\mathbf{x},t)$ can be expressed as the following asymptotic expansion forms:

$$\begin{cases} u^\varepsilon_i(\mathbf{x},t)=u^{(0)}_i(\mathbf{x},\mathbf{y},t)+\varepsilon u^{(1)}_i(\mathbf{x},\mathbf{y},t)+\varepsilon^2u^{(2)}_i(\mathbf{x},\mathbf{y},t)+\mathcal{O}(\varepsilon^3), \\ T^\varepsilon(\mathbf{x},t)=T^{(0)}(\mathbf{x},\mathbf{y},t)+\varepsilon T^{(1)}(\mathbf{x},\mathbf{y},t)+\varepsilon^2T^{(2)}(\mathbf{x},\mathbf{y},t)+\mathcal{O}(\varepsilon^3). \end{cases} \tag{2.7}$$

It is worth stressing that SOTS analysis in cylindrical coordinates is quite different from that in cartesian coordinates. Due to lack of a consistent form of $\varepsilon^\varepsilon_{ij}(\mathbf{x},t)$ in cylindrical coordinates, SOTS analysis in cylindrical coordinates should start from the basic physical quantities $\varepsilon^\varepsilon_{ij}(\mathbf{x},t)$, $\sigma^\varepsilon_{ij}(\mathbf{x},t)$ and $q^\varepsilon_i(\mathbf{x},t)$. Using (2.2), (2.6) and (2.7), the above basic physical quantities $\varepsilon^\varepsilon_{ij}(\mathbf{x},t)$ can be expanded as the following form.

$$\varepsilon^\varepsilon_{ij}(\mathbf{x},t)=\varepsilon^{-1}\varepsilon^{(-1)}_{ij}(\mathbf{x},\mathbf{y},t)+\varepsilon^0\varepsilon^{(0)}_{ij}(\mathbf{x},\mathbf{y},t)+\varepsilon^1\varepsilon^{(1)}_{ij}(\mathbf{x},\mathbf{y},t)+\mathcal{O}(\varepsilon^2), \tag{2.8}$$

https://doi.org/10.4208/cicp.OA-2016-0135 Published online by Cambridge University Press

where

$$\begin{aligned}
&\varepsilon_{ij}^{(-1)}=\frac{1}{2}\big(\widetilde{\psi}_i(u_j^{(0)})+\widetilde{\psi}_j(u_i^{(0)})\big),\ \varepsilon_{ij}^{(s)}=\varepsilon_{ij}^{(s)*}+\frac{1}{2}\big(\widetilde{\psi}_i(u_j^{(s+1)})+\widetilde{\psi}_j(u_i^{(s+1)})\big),\\
&\varepsilon_{11}^{(s)*}=\psi_1(u_1^{(s)}),\ \varepsilon_{22}^{(s)*}=\psi_2(u_2^{(s)})+\frac{u_1^{(s)}}{r},\ \varepsilon_{12}^{(s)*}=\frac{1}{2}\Big(\psi_2(u_1^{(s)})+\psi_1(u_2^{(s)})-\frac{u_2^{(s)}}{r}\Big),\\
&\varepsilon_{33}^{(s)*}=\psi_3(u_3^{(s)}),\ \varepsilon_{23}^{(s)*}=\frac{1}{2}\big(\psi_3(u_2^{(s)})+\psi_2(u_3^{(s)})\big),\ \varepsilon_{13}^{(s)*}=\frac{1}{2}\big(\psi_1(u_3^{(s)})+\psi_3(u_1^{(s)})\big),\ s=0,1.
\end{aligned}\tag{2.9}$$

Then, we start to solve the specific expanding forms of $\sigma_{ij}^{\varepsilon}(\mathbf{x},t)$ and $q_i^{\varepsilon}(\mathbf{x},t)$. Firstly, the Taylor's formula of multivariate function is given as follows:

$$f(x_0,y_0+h)=f(x_0,y_0)+f_y(x_0,y_0)h+\frac{1}{2}f_{yy}(x_0,y_0)h^2+\mathcal{O}(h^3).\tag{2.10}$$

Furthermore, the Taylor's formula (2.10) can be rewritten by multi-index notation as follows

$$f(x_0,y_0+h)=f(x_0,y_0)+\mathbf{D}^{(0,1)}f(x_0,y_0)h+\frac{1}{2}\mathbf{D}^{(0,2)}f(x_0,y_0)h^2+\mathcal{O}(h^3).\tag{2.11}$$

By means of the above-mentioned Taylor's formula and multi-index notation, the material parameters depending on temperature T^{ε} can be expanded as:

$$\begin{aligned}
C_{ijkl}^{\varepsilon}(\mathbf{x},T^{\varepsilon})&=C_{ijkl}(\mathbf{y},T^{(\varepsilon)})=C_{ijkl}(\mathbf{y},T^{(0)}+\varepsilon T^{(1)}+\varepsilon^2T^{(2)}+\mathcal{O}(\varepsilon^3))\\
&=C_{ijkl}(\mathbf{y},T^{(0)})+\mathbf{D}^{(0,1)}C_{ijkl}(\mathbf{y},T^{(0)})\big[\varepsilon T^{(1)}+\varepsilon^2T^{(2)}+\mathcal{O}(\varepsilon^3)\big]\\
&\quad+\frac{1}{2}\mathbf{D}^{(0,2)}C_{ijkl}(\mathbf{y},T^{(0)})\big[\varepsilon T^{(1)}+\varepsilon^2T^{(2)}+\mathcal{O}(\varepsilon^3)\big]^2+\cdots\\
&=C_{ijkl}(\mathbf{y},T^{(0)})+\varepsilon T^{(1)}\mathbf{D}^{(0,1)}C_{ijkl}(\mathbf{y},T^{(0)})\\
&\quad+\varepsilon^2\big[T^{(2)}\mathbf{D}^{(0,1)}C_{ijkl}(\mathbf{y},T^{(0)})+\frac{1}{2}(T^{(1)})^2\mathbf{D}^{(0,2)}C_{ijkl}(\mathbf{y},T^{(0)})\big]+\mathcal{O}(\varepsilon^3)\\
&=C_{ijkl}^{(0)}+\varepsilon C_{ijkl}^{(1)}+\varepsilon^2C_{ijkl}^{(2)}+\mathcal{O}(\varepsilon^3).
\end{aligned}\tag{2.12}$$

Using the similar expanding method as (2.12), other material parameters $c^{\varepsilon}(\mathbf{x},T^{\varepsilon})$, $\rho^{\varepsilon}(\mathbf{x},T^{\varepsilon})$, $k_{ij}^{\varepsilon}(\mathbf{x},T^{\varepsilon})$, $\beta_{ij}^{\varepsilon}(\mathbf{x},T^{\varepsilon})$ and $\vartheta_{ij}^{\varepsilon}(\mathbf{x},T^{\varepsilon})$ can be expanded as the following forms

$$\begin{aligned}
c^{\varepsilon}(\mathbf{x},T^{\varepsilon})&=c(\mathbf{y},T^{(0)})+\varepsilon T^{(1)}\mathbf{D}^{(0,1)}c(\mathbf{y},T^{(0)})\\
&\quad+\varepsilon^2\big[T^{(2)}\mathbf{D}^{(0,1)}c(\mathbf{y},T^{(0)})+\frac{1}{2}(T^{(1)})^2\mathbf{D}^{(0,2)}c(\mathbf{y},T^{(0)})\big]+\mathcal{O}(\varepsilon^3)\\
&=c^{(0)}+\varepsilon c^{(1)}+\varepsilon^2c^{(2)}+\mathcal{O}(\varepsilon^3),
\end{aligned}$$

https://doi.org/10.4208/cicp.OA-2016-0135 Published online by Cambridge University Press

$$
\begin{aligned}
\rho^{\varepsilon}(\mathbf{x},T^{\varepsilon}) &= \rho(\mathbf{y},T^{(0)})+\varepsilon T^{(1)}\mathbf{D}^{(0,1)}\rho(\mathbf{y},T^{(0)}) \\
&\quad +\varepsilon^2\big[T^{(2)}\mathbf{D}^{(0,1)}\rho(\mathbf{y},T^{(0)})+\frac{1}{2}(T^{(1)})^2\mathbf{D}^{(0,2)}\rho(\mathbf{y},T^{(0)})\big]+\mathcal{O}(\varepsilon^3) \\
&= \rho^{(0)}+\varepsilon\rho^{(1)}+\varepsilon^2\rho^{(2)}+\mathcal{O}(\varepsilon^3), \\
k_{ij}^{\varepsilon}(\mathbf{x},T^{\varepsilon}) &= k_{ij}(\mathbf{y},T^{(0)})+\varepsilon T^{(1)}\mathbf{D}^{(0,1)}k_{ij}(\mathbf{y},T^{(0)}) \\
&\quad +\varepsilon^2\big[T^{(2)}\mathbf{D}^{(0,1)}k_{ij}(\mathbf{y},T^{(0)})+\frac{1}{2}(T^{(1)})^2\mathbf{D}^{(0,2)}k_{ij}(\mathbf{y},T^{(0)})\big]+\mathcal{O}(\varepsilon^3) \\
&= k_{ij}^{(0)}+\varepsilon k_{ij}^{(1)}+\varepsilon^2 k_{ij}^{(2)}+\mathcal{O}(\varepsilon^3), \\
\beta_{ij}^{\varepsilon}(\mathbf{x},T^{\varepsilon}) &= \beta_{ij}(\mathbf{y},T^{(0)})+\varepsilon T^{(1)}\mathbf{D}^{(0,1)}\beta_{ij}(\mathbf{y},T^{(0)}) \\
&\quad +\varepsilon^2\big[T^{(2)}\mathbf{D}^{(0,1)}\beta_{ij}(\mathbf{y},T^{(0)})+\frac{1}{2}(T^{(1)})^2\mathbf{D}^{(0,2)}\beta_{ij}(\mathbf{y},T^{(0)})\big]+\mathcal{O}(\varepsilon^3) \\
&= \beta_{ij}^{(0)}+\varepsilon\beta_{ij}^{(1)}+\varepsilon^2\beta_{ij}^{(2)}+\mathcal{O}(\varepsilon^3), \\
\vartheta_{ij}^{\varepsilon}(\mathbf{x},T^{\varepsilon}) &= \vartheta_{ij}(\mathbf{y},T^{(0)})+\varepsilon T^{(1)}\mathbf{D}^{(0,1)}\vartheta_{ij}(\mathbf{y},T^{(0)}) \\
&\quad +\varepsilon^2\big([T^{(2)}\mathbf{D}^{(0,1)}\vartheta_{ij}(\mathbf{y},T^{(0)})+\frac{1}{2}(T^{(1)})^2\mathbf{D}^{(0,2)}\vartheta_{ij}(\mathbf{y},T^{(0)})\big]+\mathcal{O}(\varepsilon^3) \\
&= \vartheta_{ij}^{(0)}+\varepsilon\vartheta_{ij}^{(1)}+\varepsilon^2\vartheta_{ij}^{(2)}+\mathcal{O}(\varepsilon^3).
\end{aligned}
\tag{2.13}
$$

Similarly, the basic physical quantities $\sigma_{ij}^{\varepsilon}(\mathbf{x},t)$ and $q_i^{\varepsilon}(\mathbf{x},t)$ are expanded as following forms

$$
\begin{cases}
\sigma_{ij}^{\varepsilon}(\mathbf{x},t)=\varepsilon^{-1}\sigma_{ij}^{(-1)}(\mathbf{x},\mathbf{y},t)+\varepsilon^0\sigma_{ij}^{(0)}(\mathbf{x},\mathbf{y},t)+\varepsilon^1\sigma_{ij}^{(1)}(\mathbf{x},\mathbf{y},t)+\mathcal{O}(\varepsilon^2), \\
q_i^{\varepsilon}(\mathbf{x},t)=\varepsilon^{-1}q_i^{(-1)}(\mathbf{x},\mathbf{y},t)+\varepsilon^0 q_i^{(0)}(\mathbf{x},\mathbf{y},t)+\varepsilon^1 q_i^{(1)}(\mathbf{x},\mathbf{y},t)+\mathcal{O}(\varepsilon^2).
\end{cases}
\tag{2.14}
$$

Combining (2.3), (2.4), (2.6), (2.9), (2.12) and (2.13) together, the specific expanding forms of $\sigma_{ij}^{\varepsilon}(\mathbf{x},t)$ and $q_i^{\varepsilon}(\mathbf{x},t)$ can be derived as follows

$$
\begin{aligned}
&\sigma_{ij}^{(-1)}=C_{ijkl}^{(0)}\widetilde{\psi}_k(u_l^{(0)}),\sigma_{ij}^{(0)}=C_{ijkl}^{(1)}\widetilde{\psi}_k(u_l^{(0)})+C_{ijkl}^{(0)}\varepsilon_{kl}^{(0)*}+C_{ijkl}^{(0)}\widetilde{\psi}_k(u_l^{(1)})-\beta_{ij}^{(0)}\big(T^{(0)}-\widetilde{T}\big), \\
&\sigma_{ij}^{(1)}=C_{ijkl}^{(0)}\big(\varepsilon_{kl}^{(1)*}+\widetilde{\psi}_k(u_l^{(2)})\big)+C_{ijkl}^{(1)}\big(\varepsilon_{kl}^{(0)*}+\widetilde{\psi}_k(u_l^{(1)})\big)+C_{ijkl}^{(2)}\widetilde{\psi}_k(u_l^{(0)}) \\
&\qquad -\beta_{ij}^{(1)}\big(T^{(0)}-\widetilde{T}\big)-\beta_{ij}^{(0)}T^{(1)},
\end{aligned}
\tag{2.15}
$$

and

$$
\begin{aligned}
&q_i^{(-1)}=-k_{ij}^{(0)}\widetilde{\psi}_j(T^{(0)}),q_i^{(0)}=-k_{ij}^{(0)}\psi_j(T^{(0)})-k_{ij}^{(0)}\widetilde{\psi}_j(T^{(1)})-k_{ij}^{(1)}\widetilde{\psi}_j(T^{(0)}), \\
&q_i^{(1)}=-k_{ij}^{(0)}\psi_j(T^{(1)})-k_{ij}^{(0)}\widetilde{\psi}_j(T^{(2)})-k_{ij}^{(1)}\psi_j(T^{(0)})-k_{ij}^{(1)}\widetilde{\psi}_j(T^{(1)})-k_{ij}^{(2)}\widetilde{\psi}_j(T^{(0)}).
\end{aligned}
\tag{2.16}
$$

Then substituting (2.6), (2.12), (2.13) and (2.14) into problem (2.1), expanding the derivatives and matching terms with the same order of small periodic parameter ε, we can

https://doi.org/10.4208/cicp.OA-2016-0135 Published online by Cambridge University Press

immediately obtain

$$\begin{cases} \rho^{(0)}\dfrac{\partial^2 u_1^{(0)}}{\partial t^2}=\varepsilon^{-2}\widetilde{\psi}_j\sigma_{1j}^{(-1)}+\varepsilon^{-1}\left(\psi_j\sigma_{1j}^{(-1)}+\widetilde{\psi}_j\sigma_{1j}^{(0)}+\dfrac{\sigma_{11}^{(-1)}-\sigma_{22}^{(-1)}}{r}\right) \\ \qquad\qquad +\varepsilon^{0}\left(\psi_j\sigma_{1j}^{(0)}+\widetilde{\psi}_j\sigma_{1j}^{(1)}+\dfrac{\sigma_{11}^{(0)}-\sigma_{22}^{(0)}}{r}+f_1\right)+\mathcal{O}(\varepsilon), \\ \rho^{(0)}\dfrac{\partial^2 u_2^{(0)}}{\partial t^2}=\varepsilon^{-2}\widetilde{\psi}_j\sigma_{2j}^{(-1)}+\varepsilon^{-1}\left(\psi_j\sigma_{2j}^{(-1)}+\widetilde{\psi}_j\sigma_{2j}^{(0)}+2\dfrac{\sigma_{12}^{(-1)}}{r}\right) \\ \qquad\qquad +\varepsilon^{0}\left(\psi_j\sigma_{2j}^{(0)}+\widetilde{\psi}_j\sigma_{2j}^{(1)}+2\dfrac{\sigma_{12}^{(0)}}{r}+f_2\right)+\mathcal{O}(\varepsilon), \\ \rho^{(0)}\dfrac{\partial^2 u_3^{(0)}}{\partial t^2}=\varepsilon^{-2}\widetilde{\psi}_j\sigma_{3j}^{(-1)}+\varepsilon^{-1}\left(\psi_j\sigma_{3j}^{(-1)}+\widetilde{\psi}_j\sigma_{3j}^{(0)}+\dfrac{\sigma_{31}^{(-1)}}{r}\right) \\ \qquad\qquad +\varepsilon^{0}\left(\psi_j\sigma_{3j}^{(0)}+\widetilde{\psi}_j\sigma_{3j}^{(1)}+\dfrac{\sigma_{31}^{(0)}}{r}+f_3\right)+\mathcal{O}(\varepsilon), \\ \rho^{(0)}c^{(0)}\dfrac{\partial T^{(0)}}{\partial t}=-\varepsilon^{-2}\widetilde{\psi}_i q_i^{(-1)}-\varepsilon^{-1}\left[\psi_i q_i^{(-1)}+\widetilde{\psi}_i q_i^{(0)}+\dfrac{q_1^{(-1)}}{r}+\vartheta_{ij}^{(0)}\dfrac{\partial\varepsilon_{ij}^{(-1)}}{\partial t}\right] \\ \qquad\qquad -\varepsilon^{0}\left[\psi_i q_i^{(0)}+\widetilde{\psi}_i q_i^{(1)}+\dfrac{q_1^{(0)}}{r}+\vartheta_{ij}^{(0)}\dfrac{\partial\varepsilon_{ij}^{(0)}}{\partial t}+\vartheta_{ij}^{(1)}\dfrac{\partial\varepsilon_{ij}^{(-1)}}{\partial t}-h\right]+\mathcal{O}(\varepsilon). \end{cases} \tag{2.17}$$

From (2.17), a series of equations are derived as follows according to the classical procedure of AHM [18]

$$\mathcal{O}(\varepsilon^{-2}):\begin{cases}\widetilde{\psi}_j\sigma_{ij}^{(-1)}=0,\\ \widetilde{\psi}_i q_i^{(-1)}=0,\end{cases} \tag{2.18}$$

$$\mathcal{O}(\varepsilon^{-1}):\begin{cases}\psi_j\sigma_{1j}^{(-1)}+\widetilde{\psi}_j\sigma_{1j}^{(0)}+\dfrac{\sigma_{11}^{(-1)}-\sigma_{22}^{(-1)}}{r}=0,\\ \psi_j\sigma_{2j}^{(-1)}+\widetilde{\psi}_j\sigma_{2j}^{(0)}+2\dfrac{\sigma_{12}^{(-1)}}{r}=0,\\ \psi_j\sigma_{3j}^{(-1)}+\widetilde{\psi}_j\sigma_{3j}^{(0)}+\dfrac{\sigma_{31}^{(-1)}}{r}=0,\\ \psi_i q_i^{(-1)}+\widetilde{\psi}_i q_i^{(0)}+\dfrac{q_1^{(-1)}}{r}+\vartheta_{ij}^{(0)}\dfrac{\partial\varepsilon_{ij}^{(-1)}}{\partial t}=0,\end{cases} \tag{2.19}$$

https://doi.org/10.4208/cicp.OA-2016-0135 Published online by Cambridge University Press

$$\mathcal{O}(\varepsilon^0):\begin{cases}\rho^{(0)}\dfrac{\partial^2 u_1^{(0)}}{\partial t^2}=\psi_j\sigma_{1j}^{(0)}+\widetilde{\psi}_j\sigma_{1j}^{(1)}+\dfrac{\sigma_{11}^{(0)}-\sigma_{22}^{(0)}}{r}+f_1,\\ \rho^{(0)}\dfrac{\partial^2 u_2^{(0)}}{\partial t^2}=\psi_j\sigma_{2j}^{(0)}+\widetilde{\psi}_j\sigma_{2j}^{(1)}+2\dfrac{\sigma_{12}^{(0)}}{r}+f_2,\\ \rho^{(0)}\dfrac{\partial^2 u_3^{(0)}}{\partial t^2}=\psi_j\sigma_{3j}^{(0)}+\widetilde{\psi}_j\sigma_{3j}^{(1)}+\dfrac{\sigma_{31}^{(0)}}{r}+f_3,\\ \rho^{(0)}c^{(0)}\dfrac{\partial T^{(0)}}{\partial t}=-\psi_i q_i^{(0)}-\widetilde{\psi}_i q_i^{(1)}-\dfrac{q_1^{(0)}}{r}-\vartheta_{ij}^{(0)}\dfrac{\partial\varepsilon_{ij}^{(0)}}{\partial t}-\vartheta_{ij}^{(1)}\dfrac{\partial\varepsilon_{ij}^{(-1)}}{\partial t}+h.\end{cases}\tag{2.20}$$

Now, we start to recursively solve the asymptotic expansions terms of u_i^ε and T^ε. Firstly, substituting (2.15) and (2.16) into (2.18), the equations (2.18) can be rewritten as follows:

$$\begin{cases}\widetilde{\psi}_j\big[C_{ijkl}^{(0)}(\mathbf{y},T^{(0)})\widetilde{\psi}_k(u_l^{(0)})\big]=0,\\ \widetilde{\psi}_i\big[k_{ij}^{(0)}(\mathbf{y},T^{(0)})\widetilde{\psi}_j(T^{(0)})\big]=0.\end{cases}\tag{2.21}$$

By virtue of the periodicity of $u_i^{(0)}$ and $T^{(0)}$, and the classical theory of AHM, it is easy to acquire that $u_i^{(0)}$ and $T^{(0)}$ are independent of micro-scale variable $\mathbf{y}$, namely

$$u_i^{(0)}(\mathbf{x},\mathbf{y},t)=u_i^{(0)}(\mathbf{x},t),\quad T^{(0)}(\mathbf{x},\mathbf{y},t)=T^{(0)}(\mathbf{x},t).\tag{2.22}$$

Subsequently, (2.19) can be further simplified to the following equations by integrating (2.15), (2.16) and (2.22) together

$$\begin{cases}\widetilde{\psi}_j\big[C_{ijkl}^{(0)}(\mathbf{y},T^{(0)})\varepsilon_{kl}^{(0)*}+C_{ijkl}^{(0)}(\mathbf{y},T^{(0)})\widetilde{\psi}_k(u_l^{(1)})-\beta_{ij}^{(0)}(\mathbf{y},T^{(0)})(T^{(0)}-\widetilde{T})\big]=0,\\ \widetilde{\psi}_i\big[k_{ij}^{(0)}(\mathbf{y},T^{(0)})\psi_j(T^{(0)})+k_{ij}^{(0)}(\mathbf{y},T^{(0)})\widetilde{\psi}_j(T^{(1)})\big]=0.\end{cases}\tag{2.23}$$

Based on (2.23), we construct

$$\begin{cases}u_i^{(1)}(\mathbf{x},\mathbf{y},t)=N_i^{mn}(r,T^{(0)},\mathbf{y})\varepsilon_{mn}^{(0)*}-P_i(r,T^{(0)},\mathbf{y})(T^{(0)}-\widetilde{T}),\\ T^{(1)}(\mathbf{x},\mathbf{y},t)=M^m(r,T^{(0)},\mathbf{y})\psi_m(T^{(0)}),\ \ m,n=1,2,3,\end{cases}\tag{2.24}$$

where N_i^{mn}, P_i and M^m are the first-order auxiliary cell functions defined in unit cell Y.

Remark 2.1. It is important to mention that the first-order auxiliary cell functions are quasi-periodic functions which all depend on the macro-scale parameters r and $T^{(0)}$. r and $T^{(0)}$ play a role of a varying parameter. This is a significant difference compared to classical periodic composites with micro-scale periodicity in cartesian coordinates.

Now substituting (2.9) and (2.24) into (2.23), the following equations with homogeneous Dirichlet boundary condition are obtained after simplification and calculation

$$\begin{cases}\widetilde{\psi}_j\big[C_{ijkl}^{(0)}\widetilde{\psi}_k(N_l^{mn})\big]=-\widetilde{\psi}_j(C_{ijmn}^{(0)}), & \mathbf{y}\in Y,\\ N_l^{mn}(r,T^{(0)},\mathbf{y})=0, & \mathbf{y}\in\partial Y,\end{cases}\tag{2.25}$$

https://doi.org/10.4208/cicp.OA-2016-0135 Published online by Cambridge University Press

$$\begin{cases} \widetilde{\psi}_j\left[C_{ijkl}^{(0)}\widetilde{\psi}_k(P_l)\right]=-\widetilde{\psi}_j(\beta_{ij}^{(0)}), & \mathbf{y}\in Y, \\ P_l(r,T^{(0)},\mathbf{y})=0, & \mathbf{y}\in\partial Y, \end{cases} \tag{2.26}$$

$$\begin{cases} \widetilde{\psi}_i\left[k_{ij}^{(0)}\widetilde{\psi}_j(M^m)\right]=-\widetilde{\psi}_i(k_{im}^{(0)}), & \mathbf{y}\in Y, \\ M^m(r,T^{(0)},\mathbf{y})=0, & \mathbf{y}\in\partial Y. \end{cases} \tag{2.27}$$

Then, inspired by [12–14, 18], one can acquire the following equations by making the volume integral to both sides of (2.20) on the unit cell Y in $(\tilde{r},\tilde{\theta},\tilde{z})$ and using the Green's formula on (2.20)

$$\begin{cases} \langle\rho^{(0)}\rangle\dfrac{\partial^2 u_1^{(0)}}{\partial t^2}=\psi_j\langle\sigma_{1j}^{(0)}\rangle+\dfrac{\langle\sigma_{11}^{(0)}\rangle-\langle\sigma_{22}^{(0)}\rangle}{r}+f_1, \\ \langle\rho^{(0)}\rangle\dfrac{\partial^2 u_2^{(0)}}{\partial t^2}=\psi_j\langle\sigma_{2j}^{(0)}\rangle+2\dfrac{\langle\sigma_{12}^{(0)}\rangle}{r}+f_2, \\ \langle\rho^{(0)}\rangle\dfrac{\partial^2 u_3^{(0)}}{\partial t^2}=\psi_j\langle\sigma_{3j}^{(0)}\rangle+\dfrac{\langle\sigma_{31}^{(0)}\rangle}{r}+f_3, \\ \langle\rho^{(0)}c^{(0)}\rangle\dfrac{\partial T^{(0)}}{\partial t}=-\psi_i\langle q_i^{(0)}\rangle-\dfrac{\langle q_1^{(0)}\rangle}{r}-\left\langle\vartheta_{ij}^{(0)}\dfrac{\partial\varepsilon_{ij}^{(0)}}{\partial t}\right\rangle-\left\langle\vartheta_{ij}^{(1)}\dfrac{\partial\varepsilon_{ij}^{(-1)}}{\partial t}\right\rangle+h, \end{cases} \tag{2.28}$$

where the operators in (2.28) are defined as follows:

$$\begin{aligned} &\langle\phi(\mathbf{y})\rangle=\frac{1}{|Y|}\int_Y\phi(\mathbf{y})dY,\ \langle q_i^{(0)}\rangle=-\langle k_{im}^{(0)}+k_{ij}^{(0)}\widetilde{\psi}_j(M^m)\rangle\psi_m(T^{(0)}), \\ &\langle\sigma_{ij}^{(0)}\rangle=\langle C_{ijmn}^{(0)}+C_{ijkl}^{(0)}\widetilde{\psi}_k(N_l^{mn})\rangle\varepsilon_{mn}^{(0)*}-\langle\beta_{ij}^{(0)}+C_{ijkl}^{(0)}\widetilde{\psi}_k(P_l)\rangle(T^{(0)}-\widetilde{T}), \\ &\left\langle\vartheta_{ij}^{(0)}\frac{\partial\varepsilon_{ij}^{(0)}}{\partial t}\right\rangle=\langle\vartheta_{ij}^{(0)}+\vartheta_{mn}^{(0)}\widetilde{\psi}_n(N_m^{ij})\rangle\frac{\partial\varepsilon_{ij}^{(0)*}}{\partial t}-\langle\vartheta_{ij}^{(0)}\widetilde{\psi}_j(P_i)\rangle\frac{\partial T^{(0)}}{\partial t}. \end{aligned} \tag{2.29}$$

According to (2.28) and (2.29), the homogenized specific heat capacity $\widehat{S}$, thermal modulus $\widehat{\beta}_{ij}$, nonlinear two-way coupled tensor $\widehat{\vartheta}_{ij}$, thermal conductivity $\widehat{k}_{ij}$, mass density $\widehat{\rho}$, and elasticity coefficients $\widehat{C}_{ijmn}$ can be derived as follows

$$\begin{aligned} &\widehat{C}_{ijmn}(r,T^{(0)})=\langle C_{ijmn}^{(0)}+C_{ijkl}^{(0)}\widetilde{\psi}_l(N_k^{mn})\rangle,\widehat{\beta}_{ij}(r,T^{(0)})=\langle\beta_{ij}^{(0)}+C_{ijkl}^{(0)}\widetilde{\psi}_l(P_k)\rangle, \\ &\widehat{k}_{im}(r,T^{(0)})=\langle k_{im}^{(0)}+k_{ij}^{(0)}\widetilde{\psi}_j(M^m)\rangle,\widehat{S}(r,T^{(0)})=\langle\rho^{(0)}c^{(0)}-\vartheta_{ij}^{(0)}\widetilde{\psi}_j(P_i)\rangle, \\ &\widehat{\vartheta}_{ij}(r,T^{(0)})=\langle\vartheta_{ij}^{(0)}+\vartheta_{mn}^{(0)}\widetilde{\psi}_n(N_m^{ij})\rangle,\widehat{\rho}(T^{(0)})=\langle\rho^{(0)}\rangle. \end{aligned} \tag{2.30}$$

Further, one can define the homogenized problems attached with the same initial-

https://doi.org/10.4208/cicp.OA-2016-0135 Published online by Cambridge University Press

boundary value condition as problem (2.1)

$$\begin{cases}
\widehat{\rho}(T^{(0)})\dfrac{\partial^2 u_1^{(0)}}{\partial t^2}=\psi_j\langle\sigma_{1j}^{(0)}\rangle+\dfrac{\langle\sigma_{11}^{(0)}\rangle-\langle\sigma_{22}^{(0)}\rangle}{r}+f_1 \text{ in } \Omega\times(0,T^*),\\
\widehat{\rho}(T^{(0)})\dfrac{\partial^2 u_2^{(0)}}{\partial t^2}=\psi_j\langle\sigma_{2j}^{(0)}\rangle+2\dfrac{\langle\sigma_{12}^{(0)}\rangle}{r}+f_2 \text{ in } \Omega\times(0,T^*),\\
\widehat{\rho}(T^{(0)})\dfrac{\partial^2 u_3^{(0)}}{\partial t^2}=\psi_j\langle\sigma_{3j}^{(0)}\rangle+\dfrac{\langle\sigma_{31}^{(0)}\rangle}{r}+f_3 \text{ in } \Omega\times(0,T^*),\\
\widehat{S}(r,T^{(0)})\dfrac{\partial T^{(0)}}{\partial t}=-\psi_i\langle q_i^{(0)}\rangle-\dfrac{\langle q_1^{(0)}\rangle}{r}-\widehat{\vartheta}_{ij}(r,T^{(0)})\dfrac{\partial\varepsilon_{ij}^{(0)*}}{\partial t}+h \text{ in } \Omega\times(0,T^*),\\
\mathbf{u}^{(0)}(\mathbf{x},t)=\widehat{\mathbf{u}}(\mathbf{x},t),\ T^{(0)}(\mathbf{x},t)=\widehat{T}(\mathbf{x},t) \text{ on } \partial\Omega\times(0,T^*),\\
\mathbf{u}^{(0)}(\mathbf{x},0)=\mathbf{u}^0(\mathbf{x}),\ \dfrac{\partial\mathbf{u}^{(0)}(\mathbf{x},t)}{\partial t}\Big|_{t=0}=\mathbf{u}^1(\mathbf{x}),\ T^{(0)}(\mathbf{x},0)=\breve{T}(\mathbf{x}) \text{ in } \Omega.
\end{cases}\tag{2.31}$$

Now, we start to solve the vital second-order auxiliary cell functions. Firstly, the following equations are obtained by subtracting (2.20) from (2.31):

$$\begin{cases}
\widetilde{\psi}_j\sigma_{1j}^{(1)}=(\rho^{(0)}-\widehat{\rho})\dfrac{\partial^2 u_1^{(0)}}{\partial t^2}+\psi_j\langle\sigma_{1j}^{(0)}\rangle-\psi_j\sigma_{1j}^{(0)}+\dfrac{\langle\sigma_{11}^{(0)}\rangle-\langle\sigma_{22}^{(0)}\rangle}{r}-\dfrac{\sigma_{11}^{(0)}-\sigma_{22}^{(0)}}{r},\\
\widetilde{\psi}_j\sigma_{2j}^{(1)}=(\rho^{(0)}-\widehat{\rho})\dfrac{\partial^2 u_2^{(0)}}{\partial t^2}+\psi_j\langle\sigma_{2j}^{(0)}\rangle-\psi_j\sigma_{2j}^{(0)}+2\dfrac{\langle\sigma_{12}^{(0)}\rangle}{r}-2\dfrac{\sigma_{12}^{(0)}}{r},\\
\widetilde{\psi}_j\sigma_{3j}^{(1)}=(\rho^{(0)}-\widehat{\rho})\dfrac{\partial^2 u_3^{(0)}}{\partial t^2}+\psi_j\langle\sigma_{3j}^{(0)}\rangle-\psi_j\sigma_{3j}^{(0)}+\dfrac{\langle\sigma_{31}^{(0)}\rangle}{r}-\dfrac{\sigma_{31}^{(0)}}{r},\\
\widetilde{\psi}_i q_i^{(1)}=(\widehat{S}-\rho^{(0)}c^{(0)})\dfrac{\partial T^{(0)}}{\partial t}+\psi_i\langle q_i^{(0)}\rangle-\psi_i q_i^{(0)}+\dfrac{\langle q_1^{(0)}\rangle}{r}-\dfrac{q_1^{(0)}}{r}+\widehat{\vartheta}_{ij}\dfrac{\partial\varepsilon_{ij}^{(0)*}}{\partial t}-\vartheta_{ij}^{(0)}\dfrac{\partial\varepsilon_{ij}^{(0)}}{\partial t}.
\end{cases}\tag{2.32}$$

Secondly, the following equations can be easily gotten by combining (2.9), (2.15) and (2.24)

$$\begin{aligned}
&\vartheta_{ij}^{(0)}\varepsilon_{ij}^{(0)}=\big[\vartheta_{ij}^{(0)}+\vartheta_{mn}^{(0)}\widetilde{\psi}_n(N_m^{ij})\big]\varepsilon_{ij}^{(0)*}-\vartheta_{ij}^{(0)}\widetilde{\psi}_j(P_i)(T^{(0)}-\widetilde{T}),\\
&C_{ijkl}^{(0)}\widetilde{\psi}_k(u_l^{(1)})=C_{ijkl}^{(0)}\widetilde{\psi}_k(N_l^{mn})\varepsilon_{mn}^{(0)*}-C_{ijkl}^{(0)}\widetilde{\psi}_k(P_l)(T^{(0)}-\widetilde{T}),\\
&k_{ij}^{(0)}\widetilde{\psi}_j(T^{(1)})=k_{ij}^{(0)}\widetilde{\psi}_j(M^m)\psi_m(T^{(0)}),\\
&\varepsilon_{ij}^{(1)*}=D_{ijmn}\varepsilon_{mn}^{(0)*}+\frac{1}{2}\big[N_i^{mn}\psi_j(\varepsilon_{mn}^{(0)*})+N_j^{mn}\psi_i(\varepsilon_{mn}^{(0)*})\big]\\
&\qquad\qquad -E_{ij}(T^{(0)}-\widetilde{T})-\frac{1}{2}\big[P_i\psi_j(T^{(0)}-\widetilde{T})+P_j\psi_i(T^{(0)}-\widetilde{T})\big].
\end{aligned}\tag{2.33}$$

https://doi.org/10.4208/cicp.OA-2016-0135 Published online by Cambridge University Press

where D_{ijmn} and E_{ij} are defined as follows

$$\begin{aligned}
&D_{11mn}=\psi_1(N_1^{mn}),\ D_{22mn}=\psi_2(N_2^{mn})+\frac{N_1^{mn}}{r},\\
&D_{12mn}=\frac{1}{2}\Big[\psi_2(N_1^{mn})+\psi_1(N_2^{mn})-\frac{N_2^{mn}}{r}\Big],\ D_{33mn}=\psi_3(N_3^{mn}),\\
&D_{23mn}=\frac{1}{2}\big[\psi_3(N_2^{mn})+\psi_2(N_3^{mn})\big],\ D_{13mn}=\frac{1}{2}\big[\psi_1(N_3^{mn})+\psi_3(N_1^{mn})\big],\\
&E_{11}=\psi_1(P_1),\ E_{22}=\psi_2(P_2)+\frac{P_1}{r},\\
&E_{12}=\frac{1}{2}\Big[\psi_2(P_1)+\psi_1(P_2)-\frac{P_2}{r}\Big],\ E_{33}=\psi_3(P_3),\\
&E_{23}=\frac{1}{2}\big[\psi_3(P_2)+\psi_2(P_3)\big],\ E_{13}=\frac{1}{2}\big[\psi_1(P_3)+\psi_3(P_1)\big].
\end{aligned}\tag{2.34}$$

Then, we replace the terms $\sigma_{ij}^{(1)}$, $q_i^{(1)}$, $\langle\sigma_{ij}^{(0)}\rangle$, $\langle q_i^{(0)}\rangle$ and $\varepsilon_{ij}^{(0)}$ in (2.32) with (2.15), (2.16), (2.24), (2.29), (2.33) and (2.34). After calculation, (2.32) can be rewritten as the following two equations:

$$\begin{aligned}
&\widetilde{\psi}_j\big[C_{ijkl}^{(0)}(\mathbf{y},T^{(0)})\widetilde{\psi}_k(u_l^{(2)})\big]\\
=&(\rho^{(0)}-\widehat{\rho})\frac{\partial^2 u_i^{(0)}}{\partial t^2}-\widetilde{\psi}_j\Big(M^p\mathbf{D}^{(0,1)}C_{ijmn}^{(0)}+M^p\mathbf{D}^{(0,1)}C_{ijkl}^{(0)}\widetilde{\psi}_k(N_l^{mn})\Big)\psi_p(T^{(0)})\varepsilon_{mn}^{(0)*}\\
&+\widetilde{\psi}_j\Big(M^p\mathbf{D}^{(0,1)}\beta_{ij}^{(0)}+M^p\mathbf{D}^{(0,1)}C_{ijkl}^{(0)}\widetilde{\psi}_k(P_l)\Big)\psi_p(T^{(0)})(T^{(0)}-\widetilde{T})\\
&+\Big[\psi_j(\widehat{C}_{ijmn})-\psi_j(C_{ijmn}^{(0)})-\psi_j\big(C_{ijkl}^{(0)}\widetilde{\psi}_k(N_l^{mn})\big)-\widetilde{\psi}_j(C_{ijkl}^{(0)}D_{klmn})\Big]\varepsilon_{mn}^{(0)*}\\
&+\big[\widehat{C}_{ijmn}-C_{ijmn}^{(0)}-C_{ijkl}^{(0)}\widetilde{\psi}_k(N_l^{mn})-\widetilde{\psi}_k(C_{ikjl}^{(0)}N_l^{mn})\big]\psi_j(\varepsilon_{mn}^{(0)*})\\
&+\Big[\psi_j\big(C_{ijkl}^{(0)}\widetilde{\psi}_k(P_l)\big)-\psi_j(\widehat{\beta}_{ij})+\psi_j(\beta_{ij}^{(0)})+\widetilde{\psi}_j(C_{ijkl}^{(0)}E_{kl})\Big](T^{(0)}-\widetilde{T})\\
&+\big[\beta_{ij}^{(0)}+C_{ijkl}^{(0)}\widetilde{\psi}_k(P_l)-\widehat{\beta}_{ij}+\widetilde{\psi}_k(C_{ikjl}^{(0)}P_l)+\widetilde{\psi}_p(\beta_{ip}^{(0)}M^j)\big]\psi_j(T^{(0)}-\widetilde{T})\\
&+\frac{\delta_{i1}}{r}\Big\{\big[\widehat{C}_{11mn}-C_{11mn}^{(0)}-C_{11kl}^{(0)}\widetilde{\psi}_k(N_l^{mn})\big]\varepsilon_{mn}^{(0)*}+\big[\beta_{11}^{(0)}-\widehat{\beta}_{11}+C_{11kl}^{(0)}\widetilde{\psi}_k(P_l)\big](T^{(0)}-\widetilde{T})\Big\}\\
&-\frac{\delta_{i1}}{r}\Big\{\big[\widehat{C}_{22mn}-C_{22mn}^{(0)}-C_{22kl}^{(0)}\widetilde{\psi}_k(N_l^{mn})\big]\varepsilon_{mn}^{(0)*}+\big[\beta_{22}^{(0)}-\widehat{\beta}_{22}+C_{22kl}^{(0)}\widetilde{\psi}_k(P_l)\big](T^{(0)}-\widetilde{T})\Big\}\\
&+\frac{2\delta_{i2}}{r}\Big\{\big[\widehat{C}_{12mn}-C_{12mn}^{(0)}-C_{12kl}^{(0)}\widetilde{\psi}_k(N_l^{mn})\big]\varepsilon_{mn}^{(0)*}+\big[\beta_{12}^{(0)}-\widehat{\beta}_{12}+C_{12kl}^{(0)}\widetilde{\psi}_k(P_l)\big](T^{(0)}-\widetilde{T})\Big\}\\
&+\frac{\delta_{i3}}{r}\Big\{\big[\widehat{C}_{31mn}-C_{31mn}^{(0)}-C_{31kl}^{(0)}\widetilde{\psi}_k(N_l^{mn})\big]\varepsilon_{mn}^{(0)*}+\big[\beta_{31}^{(0)}-\widehat{\beta}_{31}+C_{31kl}^{(0)}\widetilde{\psi}_k(P_l)\big](T^{(0)}-\widetilde{T})\Big\},
\end{aligned}\tag{2.35}$$

https://doi.org/10.4208/cicp.OA-2016-0135 Published online by Cambridge University Press

$$
\begin{aligned}
&\widetilde{\psi}_i\big[k_{ij}^{(0)}(\mathbf{y},T^{(0)})\widetilde{\psi}_j(T^{(2)})\big]\\
=&-\big[\widehat{S}-\rho^{(0)}c^{(0)}+\vartheta_{ij}^{(0)}\widetilde{\psi}_j(P_i)\big]\frac{\partial T^{(0)}}{\partial t}-\big[\widehat{\vartheta}_{ij}-\vartheta_{ij}^{(0)}-\vartheta_{ij}^{(0)}\widetilde{\psi}_n(N_m^{ij})\big]\frac{\partial \varepsilon_{ij}^{(0)*}}{\partial t}\\
&-\Big[\psi_i\big(k_{ij}^{(0)}\widetilde{\psi}_j(M^m)\big)+\widetilde{\psi}_i\big(k_{ij}^{(0)}\psi_j(M^m)\big)-\psi_i(\widehat{k}_{im})+\psi_i(k_{im}^{(0)})\Big]\psi_m(T^{(0)})\\
&-\big[k_{im}^{(0)}-\widehat{k}_{im}+k_{ij}^{(0)}\widetilde{\psi}_j(M^m)+\widetilde{\psi}_j(k_{ij}^{(0)}M^m)\big]\psi_i\psi_m(T^{(0)})\\
&-\big[k_{1j}^{(0)}-\widehat{k}_{1m}+k_{1j}^{(0)}\widetilde{\psi}_j(M^m)\big]\frac{\psi_m(T^{(0)})}{r}\\
&-\widetilde{\psi}_i\Big(M^m\mathbf{D}^{(0,1)}k_{in}(\mathbf{y},T^{(0)})\Big)\psi_m(T^{(0)})\psi_n(T^{(0)})\\
&-\widetilde{\psi}_i\Big(M^m\mathbf{D}^{(0,1)}k_{ij}(\mathbf{y},T^{(0)})\widetilde{\psi}_j(M^m)\Big)\big(\psi_m(T^{(0)})\big)^2.
\end{aligned}
\tag{2.36}
$$

According to (2.35) and (2.36), we construct

$$
\begin{cases}
\begin{aligned}
u_i^{(2)}(\mathbf{x},\mathbf{y},t)=&N_i^{jmn}(r,T^{(0)},\mathbf{y})\psi_j(\varepsilon_{mn}^{(0)*})+H_i^j(r,T^{(0)},\mathbf{y})\psi_j(T^{(0)})\\
&+F_i^j(r,T^{(0)},\mathbf{y})\frac{\partial^2 u_j^{(0)}}{\partial t^2}+M_i^{mn}(r,T^{(0)},\mathbf{y})\varepsilon_{mn}^{(0)*}\\
&+Q_i(r,T^{(0)},\mathbf{y})(T^{(0)}-\widetilde{T})+W_i^{jmn}(r,T^{(0)},\mathbf{y})\psi_j(T^{(0)})\varepsilon_{mn}^{(0)*}\\
&+X_i^j(r,T^{(0)},\mathbf{y})\psi_j(T^{(0)})(T^{(0)}-\widetilde{T}),\\
T^{(2)}(\mathbf{x},\mathbf{y},t)=&S(r,T^{(0)},\mathbf{y})\frac{\partial T^{(0)}}{\partial t}+R^m(r,T^{(0)},\mathbf{y})\psi_m(T^{(0)})\\
&+M^{mn}(r,T^{(0)},\mathbf{y})\psi_m\psi_n(T^{(0)})+G^{mn}(r,T^{(0)},\mathbf{y})\frac{\partial \varepsilon_{mn}^{(0)*}}{\partial t}\\
&+A^m(r,T^{(0)},\mathbf{y})\big(\psi_m(T^{(0)})\big)^2+B^{mn}(r,T^{(0)},\mathbf{y})\psi_m(T^{(0)})\psi_n(T^{(0)}),
\end{aligned}
\end{cases}
\tag{2.37}
$$

where N_i^{jmn}, H_i^j, F_i^j, M_i^{mn}, Q_i, W_i^{jmn}, X_i^j, S, R^m, M^{mn}, G^{mn}, A^m and B^{mn} are the second-order auxiliary cell functions defined in unit cell Y. It is noticeable that second-order auxiliary cell functions in (2.37) still are quasi-periodic functions which all depend on the macro-scale parameters r and $T^{(0)}$.

Substituting (2.37) into (2.35) and (2.36) respectively, a series of equations, which are attached with the homogeneous Dirichlet boundary condition, are derived as follows:

$$
\begin{cases}
\widetilde{\psi}_p\big[C_{ipkl}^{(0)}\widetilde{\psi}_k(N_l^{jmn})\big]=\widehat{C}_{ijmn}-C_{ijmn}^{(0)}-C_{ijkl}^{(0)}\widetilde{\psi}_k(N_l^{mn})-\widetilde{\psi}_k(C_{ikjl}^{(0)}N_l^{mn}), & \mathbf{y}\in Y,\\
N_l^{jmn}(r,T^{(0)},\mathbf{y})=0, & \mathbf{y}\in\partial Y,
\end{cases}
\tag{2.38}
$$

$$
\begin{cases}
\widetilde{\psi}_p\big[C_{ipkl}^{(0)}\widetilde{\psi}_k(H_l^j)\big]=\beta_{ij}^{(0)}+C_{ijkl}^{(0)}\widetilde{\psi}_k(P_l)-\widehat{\beta}_{ij}+\widetilde{\psi}_k(C_{ikjl}^{(0)}P_l)+\widetilde{\psi}_k(\beta_{ik}^{(0)}M^j), & \mathbf{y}\in Y,\\
H_l^j(r,T^{(0)},\mathbf{y})=0, & \mathbf{y}\in\partial Y,
\end{cases}
\tag{2.39}
$$

https://doi.org/10.4208/cicp.OA-2016-0135 Published online by Cambridge University Press

$$\begin{cases} \widetilde{\psi}_p\left[C^{(0)}_{ipkl}\widetilde{\psi}_k(F^j_l)\right]=\delta_{ij}(\rho^{(0)}-\widehat{\rho}), & \mathbf{y}\in Y,\\ F^j_l(r,T^{(0)},\mathbf{y})=0, & \mathbf{y}\in\partial Y, \end{cases} \tag{2.40}$$

$$\begin{cases} \widetilde{\psi}_j\left[C^{(0)}_{ijkl}\widetilde{\psi}_k(M^{mn}_l)\right]=\psi_j(\widehat{C}_{ijmn})-\psi_j(C^{(0)}_{ijmn})-\psi_j\left[C^{(0)}_{ijkl}\widetilde{\psi}_k(N^{mn}_l)\right]-\widetilde{\psi}_j(C^{(0)}_{ijkl}D_{klmn})\\ \quad+\dfrac{\delta_{i1}}{r}\left\{\left[\widehat{C}_{11mn}-C^{(0)}_{11mn}-C^{(0)}_{11kl}\widetilde{\psi}_k(N^{mn}_l)\right]-\left[\widehat{C}_{22mn}-C^{(0)}_{22mn}-C^{(0)}_{22kl}\widetilde{\psi}_k(N^{mn}_l)\right]\right\}\\ \quad+\dfrac{2\delta_{i2}}{r}\left[\widehat{C}_{12mn}-C^{(0)}_{12mn}-C^{(0)}_{12kl}\widetilde{\psi}_k(N^{mn}_l)\right]+\dfrac{\delta_{i3}}{r}\left[\widehat{C}_{31mn}-C^{(0)}_{31mn}-C^{(0)}_{31kl}\widetilde{\psi}_k(N^{mn}_l)\right], & \mathbf{y}\in Y,\\ M^{mn}_l(r,T^{(0)},\mathbf{y})=0, & \mathbf{y}\in\partial Y, \end{cases} \tag{2.41}$$

$$\begin{cases} \widetilde{\psi}_j\left[C^{(0)}_{ijkl}\widetilde{\psi}_k(Q_l)\right]=\psi_j\left(C^{(0)}_{ijkl}\widetilde{\psi}_k(P_l)\right)-\psi_j(\widehat{\beta}_{ij})+\psi_j(\beta^{(0)}_{ij})+\widetilde{\psi}_j(C^{(0)}_{ijkl}E_{kl})\\ \qquad+\dfrac{\delta_{i1}}{r}\left\{\left[\beta^{(0)}_{11}-\widehat{\beta}_{11}+C^{(0)}_{11kl}\widetilde{\psi}_k(P_l)\right]-\left[\beta^{(0)}_{22}-\widehat{\beta}_{22}+C^{(0)}_{22kl}\widetilde{\psi}_k(P_l)\right]\right\}\\ \qquad+\dfrac{2\delta_{i2}}{r}\left[\beta^{(0)}_{12}-\widehat{\beta}_{12}+C^{(0)}_{12kl}\widetilde{\psi}_k(P_l)\right]+\dfrac{\delta_{i3}}{r}\left[\beta^{(0)}_{31}-\widehat{\beta}_{31}+C^{(0)}_{31kl}\widetilde{\psi}_k(P_l)\right], & \mathbf{y}\in Y,\\ Q_l(r,T^{(0)},\mathbf{y})=0, & \mathbf{y}\in\partial Y, \end{cases} \tag{2.42}$$

$$\begin{cases} \widetilde{\psi}_p\left[C^{(0)}_{ipkl}\widetilde{\psi}_k(W^{jmn}_l)\right]=-\widetilde{\psi}_p\left[M^j\mathbf{D}^{(0,1)}C^{(0)}_{ipmn}+M^j\mathbf{D}^{(0,1)}C^{(0)}_{ipkl}\widetilde{\psi}_k(N^{mn}_l)\right], & \mathbf{y}\in Y,\\ W^{jmn}_l(r,T^{(0)},\mathbf{y})=0, & \mathbf{y}\in\partial Y, \end{cases} \tag{2.43}$$

$$\begin{cases} \widetilde{\psi}_p\left[C^{(0)}_{ipkl}\widetilde{\psi}_k(X^j_l)\right]=\widetilde{\psi}_p\left[M^j\mathbf{D}^{(0,1)}\beta^{(0)}_{ip}+M^j\mathbf{D}^{(0,1)}C^{(0)}_{ipkl}\widetilde{\psi}_k(P_l)\right], & \mathbf{y}\in Y,\\ X^j_l(r,T^{(0)},\mathbf{y})=0, & \mathbf{y}\in\partial Y, \end{cases} \tag{2.44}$$

$$\begin{cases} \widetilde{\psi}_i\left[k^{(0)}_{ij}\widetilde{\psi}_j(S)\right]=-\left[\widehat{S}-\rho^{(0)}c^{(0)}+\vartheta^{(0)}_{ij}\widetilde{\psi}_j(P_i)\right], & \mathbf{y}\in Y,\\ S(r,T^{(0)},\mathbf{y})=0, & \mathbf{y}\in\partial Y, \end{cases} \tag{2.45}$$

$$\begin{cases} \widetilde{\psi}_i\left[k^{(0)}_{ij}\widetilde{\psi}_j(R^m)\right]=-\left[\psi_i\left(k^{(0)}_{ij}\widetilde{\psi}_j(M^m)\right)+\widetilde{\psi}_i\left(k^{(0)}_{ij}\psi_j(M^m)\right)-\psi_i(\widehat{k}_{im})+\psi_i(k^{(0)}_{im})\right]\\ \qquad\qquad-\dfrac{\left[k^{(0)}_{1m}-\widehat{k}_{1m}+k^{(0)}_{1j}\widetilde{\psi}_j(M^m)\right]}{r}, & \mathbf{y}\in Y,\\ R^m(r,T^{(0)},\mathbf{y})=0, & \mathbf{y}\in\partial Y, \end{cases} \tag{2.46}$$

$$\begin{cases} \widetilde{\psi}_i\left[k^{(0)}_{ij}\widetilde{\psi}_j(M^{mn})\right]=-\left[k^{(0)}_{mn}-\widehat{k}_{mn}+k^{(0)}_{mj}\widetilde{\psi}_j(M^n)+\widetilde{\psi}_j(k^{(0)}_{mj}M^n)\right], & \mathbf{y}\in Y,\\ M^{mn}(r,T^{(0)},\mathbf{y})=0, & \mathbf{y}\in\partial Y, \end{cases} \tag{2.47}$$

$$\begin{cases} \widetilde{\psi}_i\left[k^{(0)}_{ij}\widetilde{\psi}_j(G^{mn})\right]=-\left[\widehat{\vartheta}_{mn}-\vartheta^{(0)}_{mn}-\vartheta^{(0)}_{ij}\widetilde{\psi}_j(N^{mn}_i)\right], & \mathbf{y}\in Y,\\ G^{mn}(r,T^{(0)},\mathbf{y})=0, & \mathbf{y}\in\partial Y, \end{cases} \tag{2.48}$$

https://doi.org/10.4208/cicp.OA-2016-0135 Published online by Cambridge University Press

$$\begin{cases} \widetilde{\psi}_i\left[k_{ij}^{(0)}\widetilde{\psi}_j(A^m)\right] = -\widetilde{\psi}_i\left[M^m\mathbf{D}^{(0,1)}k_{ij}^{(0)}(\mathbf{y},T^{(0)})\widetilde{\psi}_j(M^m)\right], & \mathbf{y}\in Y, \\ A^m(r,T^{(0)},\mathbf{y}) = 0, & \mathbf{y}\in\partial Y, \end{cases} \tag{2.49}$$

$$\begin{cases} \widetilde{\psi}_i\left[k_{ij}^{(0)}\widetilde{\psi}_j(B^{mn})\right] = -\widetilde{\psi}_i\left[M^m\mathbf{D}^{(0,1)}k_{in}^{(0)}(\mathbf{y},T^{(0)})\right], & \mathbf{y}\in Y, \\ B^{mn}(r,T^{(0)},\mathbf{y}) = 0, & \mathbf{y}\in\partial Y, \end{cases} \tag{2.50}$$

where $p=1,2,3$.

Remark 2.2. According to Lax-Milgram theorem and the hypotheses (A)-(C), it is easy to prove that problems (2.25)-(2.27) and (2.38)-(2.50) have a unique solution for any fixed macro-scale parameters r and $T^{(0)}$ except for problems (2.40), (2.41) and (2.45). With regard to problems (2.41), (2.42) and (2.46), they have a unique solution for any fixed macro-scale variable (r,θ,z). The difference between these two kinds of auxiliary cell functions is because there exist $\psi_j(\widehat{C}_{ijmn})$, $\psi_j(\widehat{\beta}_{ij})$ and $\psi_i(\widehat{k}_{im})$ in right sides of problems (2.41), (2.42) and (2.46), respectively.

In conclusion, the following theorem is obtained based on SOTS analysis in this subsection for multiscale problem (2.1).

Theorem 2.1. *The nonlinear dynamic thermo-mechanical problem* (2.1) *of composites with periodic configurations in cylindrical coordinates has SOTS asymptotic expansion solutions as follows*

$$\begin{aligned} u_i^\varepsilon(\mathbf{x},t) \cong u_i^{(0)} &+ \varepsilon\left[N_i^{mn}(r,T^{(0)},\mathbf{y})\varepsilon_{mn}^{(0)*} - P_i(r,T^{(0)},\mathbf{y})(T^{(0)}-\widetilde{T})\right] \\ &+ \varepsilon^2\Bigg[N_i^{jmn}(r,T^{(0)},\mathbf{y})\psi_j(\varepsilon_{mn}^{(0)*}) + H_i^j(r,T^{(0)},\mathbf{y})\psi_j(T^{(0)}) \\ &+ F_i^j(r,T^{(0)},\mathbf{y})\frac{\partial^2 u_j^{(0)}}{\partial t^2} + M_i^{mn}(r,T^{(0)},\mathbf{y})\varepsilon_{mn}^{(0)*} + Q_i(r,T^{(0)},\mathbf{y})(T^{(0)}-\widetilde{T}) \\ &+ W_i^{jmn}(r,T^{(0)},\mathbf{y})\psi_j(T^{(0)})\varepsilon_{mn}^{(0)*} + X_i^j(r,T^{(0)},\mathbf{y})\psi_j(T^{(0)})(T^{(0)}-\widetilde{T})\Bigg], \end{aligned} \tag{2.51}$$

$$\begin{aligned} T^\varepsilon(\mathbf{x},t) \cong T^{(0)} &+ \varepsilon M^m(r,T^{(0)},\mathbf{y})\psi_m(T^{(0)}) + \varepsilon^2\Bigg[M^{mn}(r,T^{(0)},\mathbf{y})\psi_m\psi_n(T^{(0)}) \\ &+ S(r,T^{(0)},\mathbf{y})\frac{\partial T^{(0)}}{\partial t} + R^m(r,T^{(0)},\mathbf{y})\psi_m(T^{(0)}) + G^{mn}(r,T^{(0)},\mathbf{y})\frac{\partial \varepsilon_{mn}^{(0)*}}{\partial t} \\ &+ A^m(r,T^{(0)},\mathbf{y})\left(\psi_m(T^{(0)})\right)^2 + B^{mn}(r,T^{(0)},\mathbf{y})\psi_m(T^{(0)})\psi_n(T^{(0)})\Bigg], \end{aligned} \tag{2.52}$$

where $u_i^{(0)}$ and $T^{(0)}$ are the solutions of the homogenized problem (2.31)*, and N_i^{mn}, P_i, M^m are the first-order auxiliary cell functions defined by* (2.25)-(2.27)*, N_i^{jmn}, H_i^j, F_i^j, M_i^{mn}, Q_i, W_i^{jmn}, X_i^j, S, R^m, M^{mn}, G^{mn}, A^m and B^{mn} are the second-order auxiliary cell functions defined by* (2.38)-(2.50).

https://doi.org/10.4208/cicp.OA-2016-0135 Published online by Cambridge University Press

It stressed that it is easy to acquire the strains, stresses and heat fluxes of multiscale problems (2.1) once we get the high-precision SOTS solutions for the displacement fields and temperature field of multiscale problems (2.1). Besides, it should be stressed that the homogenization is not stable, i.e. the homogenized problem (2.31) is not exactly of the same form with the heterogeneous one (2.1) (for instance, the homogenized specific heat coefficient cannot be defined, hidden in the homogenized specific heat capacity).

2.2 Error analysis in the pointwise sense

In this subsection, the specific error analysis of FOTS solutions and SOTS solutions in the pointwise sense is given. Firstly, we denote the FOTS solutions and SOTS solutions for the governing equations as follows:

$$\begin{aligned} &u_i^{(1\varepsilon)}=u_i^{(0)}+\varepsilon u_i^{(1)},\quad T^{(1\varepsilon)}=T^{(0)}+\varepsilon T^{(1)},\\ &u_i^{(2\varepsilon)}=u_i^{(0)}+\varepsilon u_i^{(1)}+\varepsilon^2 u_i^{(2)},\quad T^{(2\varepsilon)}=T^{(0)}+\varepsilon T^{(1)}+\varepsilon^2 T^{(2)}. \end{aligned} \tag{2.53}$$

Then, let

$$\begin{aligned} &u_{\Delta i}^{(1\varepsilon)}=u_i^{\varepsilon}-u_i^{(1\varepsilon)},\quad T_\Delta^{(1\varepsilon)}=T^{\varepsilon}-T^{(1\varepsilon)},\\ &u_{\Delta i}^{(2\varepsilon)}=u_i^{\varepsilon}-u_i^{(2\varepsilon)},\quad T_\Delta^{(2\varepsilon)}=T^{\varepsilon}-T^{(2\varepsilon)}. \end{aligned} \tag{2.54}$$

Before giving the detailed analysis procedure, we need to make some assumptions about multiscale problem (2.1). Suppose that Ω is the union of the entire periodic cells, i.e. $\bar{\Omega}=\cup_{\mathbf{z}\in T_\varepsilon}\varepsilon(\mathbf{z}+\bar{Y})$, where the index set $T_\varepsilon=\{\mathbf{z}=(z_1,z_2,z_3)\in Z^3,\varepsilon(\mathbf{z}+\bar{Y})\subset\bar{\Omega}\}$. Besides, let $E_{\mathbf{z}}=\varepsilon(\mathbf{z}+Y)$ and $\partial E_{\mathbf{z}}$ be the boundary of $E_{\mathbf{z}}$. After that, substituting $u_{\Delta i}^{(1\varepsilon)}$ and $T_\Delta^{(1\varepsilon)}$ of (2.54) into (2.1) and using (2.25)-(2.27), (2.31), the following residual equation of FOTS solutions are obtained, which holds in the distribution sense:

$$\begin{cases} \rho^\varepsilon\dfrac{\partial^2 u_{\Delta i}^{(1\varepsilon)}}{\partial t^2}-\Big\{\psi_j\sigma_{ij}^\varepsilon(\mathbf{u}_\Delta^{(1\varepsilon)},T_\Delta^{(1\varepsilon)})+\delta_{i1}\Big[\dfrac{\sigma_{11}^\varepsilon(\mathbf{u}_\Delta^{(1\varepsilon)},T_\Delta^{1\varepsilon})-\sigma_{22}^\varepsilon(\mathbf{u}_\Delta^{(1\varepsilon)},T_\Delta^{(1\varepsilon)})}{r}\Big]\\ \qquad\qquad+\delta_{i2}\dfrac{2\sigma_{12}^\varepsilon(\mathbf{u}_\Delta^{(1\varepsilon)},T_\Delta^{(1\varepsilon)})}{r}+\delta_{i3}\dfrac{\sigma_{31}^\varepsilon(\mathbf{u}_\Delta^{(1\varepsilon)},T_\Delta^{(1\varepsilon)})}{r}\Big\}\\ \qquad=S_{0i}(\mathbf{x},\mathbf{y},t)+\varepsilon S_{1i}(\mathbf{x},\mathbf{y},t)\ \text{ in }\Omega\times(0,T^*),\\ \rho^\varepsilon c^\varepsilon\dfrac{\partial T_\Delta^{(1\varepsilon)}}{\partial t}+\Big[\psi_i q_i^\varepsilon(T_\Delta^{(1\varepsilon)})+\dfrac{q_1^\varepsilon(T_\Delta^{(1\varepsilon)})}{r}+\vartheta_{ij}^\varepsilon\dfrac{\partial\varepsilon_{ij}^\varepsilon(\mathbf{u}_\Delta^{(1\varepsilon)})}{\partial t}\Big]\\ \qquad=F_0(\mathbf{x},\mathbf{y},t)+\varepsilon F_1(\mathbf{x},\mathbf{y},t)\ \text{ in }\Omega\times(0,T^*),\\ \mathbf{u}_\Delta^{(1\varepsilon)}(\mathbf{x},t)=\mathbf{0},\ T_\Delta^{(1\varepsilon)}(\mathbf{x},t)=0\ \text{ on }\partial\Omega\times(0,T^*),\\ u_{\Delta i}^{(1\varepsilon)}(\mathbf{x},0)=-\varepsilon N_i^{mn}\varepsilon_{mn}^{(0)*}\big(\mathbf{u}^0(\mathbf{x})\big)+\varepsilon P_i(\breve{T}(\mathbf{x})-\widetilde{T})=\varepsilon\widehat{\psi}_{1i}(\mathbf{x}),\\ \dfrac{\partial u_{\Delta i}^{(1\varepsilon)}}{\partial t}\Big|_{t=0}=-\varepsilon N_i^{mn}\varepsilon_{mn}^{(0)*}\big(\mathbf{u}^1(\mathbf{x})\big)+\varepsilon P_i\dfrac{\partial T^{(0)}}{\partial t}\Big|_{t=0}=\varepsilon\widehat{\psi}_{2i}(\mathbf{x}),\\ T_\Delta^{(1\varepsilon)}(\mathbf{x},0)=-\varepsilon M^m\psi_m\big(\breve{T}(\mathbf{x})\big)=\varepsilon\widehat{\psi}_3(\mathbf{x})\ \text{ in }\Omega, \end{cases} \tag{2.55}$$

https://doi.org/10.4208/cicp.OA-2016-0135 Published online by Cambridge University Press

where the operators $\sigma_{ij}^{\varepsilon}(\mathbf{u}_{\Delta}^{(1\varepsilon)},T_{\Delta}^{(1\varepsilon)})=C_{ijkl}^{\varepsilon}\varepsilon_{kl}^{\varepsilon}(\mathbf{u}_{\Delta}^{(1\varepsilon)})-\beta_{ij}^{\varepsilon}T_{\Delta}^{(1\varepsilon)}$ and $q_i^{\varepsilon}(T_{\Delta}^{(1\varepsilon)})=-k_{ij}^{\varepsilon}\psi_j(T_{\Delta}^{(1\varepsilon)})$. Moreover, the detailed forms of $S_{0i}(\mathbf{x},\mathbf{y},t)$, $S_{1i}(\mathbf{x},\mathbf{y},t)$, $F_0(\mathbf{x},\mathbf{y},t)$ and $F_1(\mathbf{x},\mathbf{y},t)$ are given in Appendix A.

Furthermore, substituting $u_{\Delta i}^{(2\varepsilon)}$ and $T_{\Delta}^{(2\varepsilon)}$ of (2.54) into (2.1) and using (2.25)-(2.27), (2.31), (2.38)-(2.50), the following residual equation of SOTS solutions are obtained, which also holds in the distribution sense:

$$
\begin{cases}
\rho^{\varepsilon}\dfrac{\partial^2 u_{\Delta i}^{(2\varepsilon)}}{\partial t^2}-\Big\{\psi_j\sigma_{ij}^{\varepsilon}(\mathbf{u}_{\Delta}^{(2\varepsilon)},T_{\Delta}^{(2\varepsilon)})+\delta_{i1}\Big[\dfrac{\sigma_{11}^{\varepsilon}(\mathbf{u}_{\Delta}^{(2\varepsilon)},T_{\Delta}^{(2\varepsilon)})-\sigma_{22}^{\varepsilon}(\mathbf{u}_{\Delta}^{(2\varepsilon)},T_{\Delta}^{(2\varepsilon)})}{r}\Big]\\
\qquad\qquad+\delta_{i2}\dfrac{2\sigma_{12}^{\varepsilon}(\mathbf{u}_{\Delta}^{(2\varepsilon)},T_{\Delta}^{(2\varepsilon)})}{r}+\delta_{i3}\dfrac{\sigma_{31}^{\varepsilon}(\mathbf{u}_{\Delta}^{(2\varepsilon)},T_{\Delta}^{(2\varepsilon)})}{r}\Big\}\\
\qquad=\varepsilon H_i(\mathbf{x},\mathbf{y},t)\ \text{ in }\Omega\times(0,T^*),\\
\rho^{\varepsilon}c^{\varepsilon}\dfrac{\partial T_{\Delta}^{(2\varepsilon)}}{\partial t}+\Big[\psi_i q_i^{\varepsilon}(T_{\Delta}^{(2\varepsilon)})+\dfrac{q_1^{\varepsilon}(T_{\Delta}^{(2\varepsilon)})}{r}+\vartheta_{ij}^{\varepsilon}\dfrac{\partial\varepsilon_{ij}^{\varepsilon}(\mathbf{u}_{\Delta}^{(2\varepsilon)})}{\partial t}\Big]\\
\qquad=\varepsilon G(\mathbf{x},\mathbf{y},t)\ \text{ in }\Omega\times(0,T^*),\\
\mathbf{u}_{\Delta}^{(2\varepsilon)}(\mathbf{x},t)=\mathbf{0},\ \ T_{\Delta}^{(2\varepsilon)}(\mathbf{x},t)=0\ \text{ on }\partial\Omega\times(0,T^*),\\
u_{\Delta i}^{(2\varepsilon)}(\mathbf{x},0)=-\varepsilon\Big[N_i^{mn}\varepsilon_{mn}^{(0)*}(\mathbf{u}^0(\mathbf{x}))-P_i(\check{T}(\mathbf{x})-\widetilde{T})\Big]-\varepsilon^2\Big\{N_i^{jmn}\psi_j\Big[\varepsilon_{mn}^{(0)*}(\mathbf{u}^0(\mathbf{x}))\Big]\\
\qquad+H_i^j\psi_j(\check{T}(\mathbf{x}))+F_i^j\dfrac{\partial^2 u_j^{(0)}}{\partial t^2}+M_i^{mn}\varepsilon_{mn}^{(0)*}(\mathbf{u}^0(\mathbf{x}))+Q_i(\check{T}(\mathbf{x})-\widetilde{T})\\
\qquad+W_i^{jmn}\psi_j(\check{T}(\mathbf{x}))\varepsilon_{mn}^{(0)*}(\mathbf{u}^0(\mathbf{x}))+X_i^j\psi_j(\check{T}(\mathbf{x}))(\check{T}(\mathbf{x})-\widetilde{T})\Big\}=\varepsilon\widetilde{\psi}_{1i}(\mathbf{x}),\\
\dfrac{\partial u_{\Delta i}^{(2\varepsilon)}}{\partial t}\Big|_{t=0}=-\varepsilon\Big[N_i^{mn}\varepsilon_{mn}^{(0)*}(\mathbf{u}^1(\mathbf{x}))-P_i\dfrac{\partial T^{(0)}}{\partial t}\Big|_{t=0}\Big]-\varepsilon^2\Big\{N_i^{jmn}\psi_j\Big[\varepsilon_{mn}^{(0)*}(\mathbf{u}^1(\mathbf{x}))\Big]\\
\qquad+H_i^j\dfrac{\partial\psi_j(T^{(0)})}{\partial t}\Big|_{t=0}+F_i^j\dfrac{\partial^3 u_j^{(0)}}{\partial t^3}\Big|_{t=0}+M_i^{mn}\varepsilon_{mn}^{(0)*}(\mathbf{u}^1(\mathbf{x}))+Q_i\dfrac{\partial T^{(0)}}{\partial t}\Big|_{t=0}\\
\qquad+W_i^{jmn}\dfrac{\partial\psi_j(T^{(0)})\varepsilon_{mn}^{(0)*}}{\partial t}\Big|_{t=0}+X_i^j\dfrac{\partial\psi_j(T^{(0)})(T^{(0)}-\widetilde{T})}{\partial t}\Big|_{t=0}\Big\}=\varepsilon\widetilde{\psi}_{2i}(\mathbf{x}),\\
T_{\Delta}^{(2\varepsilon)}(\mathbf{x},0)=-\varepsilon M^m\psi_m(\check{T}(\mathbf{x}))-\varepsilon^2\Big[S\dfrac{\partial T^{(0)}}{\partial t}\Big|_{t=0}+R^m\psi_m(\check{T}(\mathbf{x}))+M^{mn}\psi_m\psi_n(\check{T}(\mathbf{x}))\\
\qquad+G^{mn}\varepsilon_{mn}^{(0)*}(\mathbf{u}^1(\mathbf{x}))+A^m(\psi_m(\check{T}(\mathbf{x})))^2+B^{mn}\psi_m(\check{T}(\mathbf{x}))\psi_n(\check{T}(\mathbf{x}))\Big]=\varepsilon\widetilde{\psi}_3(\mathbf{x})\ \text{ in }\Omega,
\end{cases}
\tag{2.56}
$$

where the specific forms of $H_i(\mathbf{x},\mathbf{y},t)$ and $G(\mathbf{x},\mathbf{y},t)$ also are listed in Appendix A.

Now we can give a conclusion about the error analysis in the pointwise sense. From the residual equation (2.55), one can easily find that the residual of FOTS solutions is order $\mathcal{O}(1)$ in the pointwise sense due to the terms $S_{0i}(\mathbf{x},\mathbf{y},t)$ and $F_0(\mathbf{x},\mathbf{y},t)$. In addition, it is clear to see that the residual of SOTS solutions is order $\mathcal{O}(\varepsilon)$ in the pointwise sense

https://doi.org/10.4208/cicp.OA-2016-0135 Published online by Cambridge University Press

from the residual equation (2.56). This means that SOTS solutions can satisfy the original equation (2.1) in the pointwise sense. Thus even ε is a small constant, the SOTS solutions can still provide the required accuracy for engineering computation and capture the micro-scale oscillating behavior of composite materials. This is the main reason and motivation to develop the SOTS solutions.

3 Second-order two-scale numerical algorithm

In this section, we give the SOTS numerical algorithm for the governing problem (2.1), which is based on the FDM in time direction and the FEM in spatial region. The detailed algorithm procedures for two-dimensional and three-dimensional multiscale problem (2.1) are listed as follows:

(1) Define the geometric structure of the unit cell $Y=(0,1)^{\mathcal{N}}(\mathcal{N}=2,3)$ and homogenized macroscopic region Ω in $\mathbb{R}^{\mathcal{N}}$, and verify the material parameters of composite materials. Then, generate the triangular finite element mesh for two-dimensional problems or tetrahedral mesh for three-dimensional problems. Let $J^{h_1}=\{K\}$ and $J^{h_0}=\{e\}$ be a regular family of triangles or tetrahedra of the unit cell Y and the homogenized macroscopic region Ω, respectively, where $h_1=\max_K\{h_K\}$ and $h_0=\max_e\{h_e\}$. And define the linear conforming finite element spaces $V_{h_1}(Y)=\{\nu\in C^0(\bar{Y}):\nu|_{\partial Y}=0,\nu|_K\in P_1(K)\}\subset H_0^1(Y)$ and $V_{h_0}(\Omega)=\{\nu\in C^0(\bar{\Omega}):\nu|_{\partial\Omega}=0,\nu|_e\in P_1(e)\}\subset H_0^1(\Omega)$ for the above two regions, respectively.

(2) Solve the first-order auxiliary cell functions (2.25)-(2.27) on $V_{h_1}(Y)$ corresponding to different representative macro-scale parameters $(r_{s_1},T_{s_2})\in[r_{\min},r_{\max}]\times[T_{\min},T_{\max}]$, where $s_1,s_2=1,2,\cdots,\bar{L}(\bar{L}\in\mathbf{N}^*)$. And the homogenized material parameters $\widehat{\rho}$, $\widehat{C}_{ijmn}$, $\widehat{\beta}_{ij}$, $\widehat{\vartheta}_{ij}$, $\widehat{S}$ and $\widehat{k}_{ij}$ are evaluated by making integral of (2.30) corresponding to different macro-scale parameters (r_{s_1},T_{s_2}). After that, the homogenized material parameters can be calculated by interpolation method on each nodes of $V_{h_0}(\Omega)$.

(3) Compute the homogenized problem (2.31) by coupled FDM-FEM method in a coarse mesh and with a large time step on the whole domain $\Omega\times(0,T^*)$. Using the uniform time step $\Delta t=\frac{T^*}{M}$ to discretize time-domain $(0,T^*)$ as $0=t_0<t_1<\cdots<t_M=T^*$ and $t_N=N\Delta t$ $(N=0,\cdots,M)$, then we denote $f_i^N=f_i(\mathbf{x},t_N)$. It is easy to know that the dynamic system (2.31) is a strongly coupled nonlinear system. In order to maintain the unconditional stability of our SOTS numerical algorithm, the implicit FDM scheme is employed in time domain and FEM is adopted in spatial domain. The concrete

https://doi.org/10.4208/cicp.OA-2016-0135 Published online by Cambridge University Press

FDM-FEM scheme for homogenized problem (2.31) is given as follows:

$$\begin{cases} \displaystyle\int_\Omega \widehat{\rho}(T^{(0),N+1})\frac{u_i^{(0),N+1}-2u_i^{(0),N}+u_i^{(0),N-1}}{(\Delta t)^2}\nu_i^{h_0}rd\Omega \\ \qquad\qquad +\displaystyle\int_\Omega \widehat{C}_{ijkl}(r,T^{(0),N+1})\varepsilon_{kl}^{(0)*}(\mathbf{u}^{(0),N+1})\varepsilon_{ij}^{(0)*}(\boldsymbol{\nu}^{h_0})rd\Omega \\ \qquad\qquad -\displaystyle\int_\Omega \widehat{\beta}_{ij}(r,T^{(0),N+1})(T^{(0),N+1}-\widetilde{T})\varepsilon_{ij}^{(0)*}(\boldsymbol{\nu}^{h_0})rd\Omega \\ \qquad =\displaystyle\int_\Omega f_i^{N+1}\nu_i^{h_0}rd\Omega, \forall \boldsymbol{\nu}^{h_0}\in\left(V_{h_0}(\Omega)\right)^{\mathcal{N}}, \\ \displaystyle\int_\Omega \widehat{S}(r,T^{(0),N+1})\frac{T^{(0),N+1}-T^{(0),N}}{\Delta t}\widetilde{\varphi}^{h_0}rd\Omega \\ \qquad\qquad +\displaystyle\int_\Omega \widehat{k}_{ij}(r,T^{(0),N+1})\psi_j(T^{(0),N+1})\psi_i(\widetilde{\varphi}^{h_0})rd\Omega \\ \qquad\qquad +\displaystyle\int_\Omega \widehat{\vartheta}_{ij}(r,T^{(0),N+1})\frac{\varepsilon_{ij}^{(0)*}(\mathbf{u}^{(0),N+1})-\varepsilon_{ij}^{(0)*}(\mathbf{u}^{(0),N})}{\Delta t}\widetilde{\varphi}^{h_0}rd\Omega \\ \qquad =\displaystyle\int_\Omega h^{N+1}\widetilde{\varphi}^{h_0}rd\Omega, \forall\widetilde{\varphi}^{h_0}\in V_{h_0}(\Omega). \end{cases} \tag{3.1}$$

It should be noted that, system (3.1) is a nonlinear system which can't be computed directly. Hence, we present the following direct iteration method for solving nonlinear system (3.1):

Step 1: Let $T_0(\mathbf{x})$ be the initial function, and $T_\lambda(\mathbf{x})$ and $\mathbf{u}_\lambda(\mathbf{x})$ be the solutions of the λ-th iterative step, $\lambda\geq 1$. Set the iteration threshold as E_{tol} and $\widehat{E}_{tol}$, respectively, and begin iterating.

Step 2: At the λ-th iteration step, use $T_{\lambda-1}(\mathbf{x})$ to linearize the problem (3.1) as follows:

$$\begin{cases} \displaystyle\int_\Omega \widehat{\rho}(T_{\lambda-1})\frac{u_{i,\lambda}-2u_i^{(0),N}+u_i^{(0),N-1}}{(\Delta t)^2}\nu_i^{h_0}rd\Omega \\ \qquad\qquad +\displaystyle\int_\Omega \widehat{C}_{ijkl}(r,T_{\lambda-1})\varepsilon_{kl}^{(0)*}(\mathbf{u}_\lambda)\varepsilon_{ij}^{(0)*}(\boldsymbol{\nu}^{h_0})rd\Omega \\ \qquad -\displaystyle\int_\Omega \widehat{\beta}_{ij}(r,T_{\lambda-1})(T_\lambda-\widetilde{T})\varepsilon_{ij}^{(0)*}(\boldsymbol{\nu}^{h_0})rd\Omega \\ \qquad =\displaystyle\int_\Omega f_i^{N+1}\nu_i^{h_0}rd\Omega, \forall \boldsymbol{\nu}^{h_0}\in\left(V_{h_0}(\Omega)\right)^{\mathcal{N}}, \\ \displaystyle\int_\Omega \widehat{S}(r,T_{\lambda-1})\frac{T_\lambda-T^{(0),N}}{\Delta t}\widetilde{\varphi}^{h_0}rd\Omega \\ \qquad\qquad +\displaystyle\int_\Omega \widehat{k}_{ij}(r,T_{\lambda-1})\psi_j(T_\lambda)\psi_i(\widetilde{\varphi}^{h_0})rd\Omega \\ \qquad\qquad +\displaystyle\int_\Omega \widehat{\vartheta}_{ij}(r,T_{\lambda-1})\frac{\varepsilon_{ij}^{(0)*}(\mathbf{u}_\lambda)-\varepsilon_{ij}^{(0)*}(\mathbf{u}^{(0),N})}{\Delta t}\widetilde{\varphi}^{h_0}rd\Omega \\ \qquad =\displaystyle\int_\Omega h^{N+1}\widetilde{\varphi}^{h_0}rd\Omega, \forall\widetilde{\varphi}^{h_0}\in V_{h_0}(\Omega). \end{cases} \tag{3.2}$$

https://doi.org/10.4208/cicp.OA-2016-0135 Published online by Cambridge University Press

Step 3: If $||T_\lambda(\mathbf{x})-T_{\lambda-1}(\mathbf{x})||_{L^\infty(\Omega)} \le E_{tol}$ and $||\mathbf{u}_\lambda(\mathbf{x})-\mathbf{u}_{\lambda-1}(\mathbf{x})||_{L^\infty(\Omega)} \le \widehat{E}_{tol}$, stop; otherwise $\lambda=\lambda+1$, go back to Step 2.

Step 4: Set $T^{(0),N+1}=T_{sat}$ and $\mathbf{u}^{(0),N+1}=\mathbf{u}_{sat}$, where T_{sat} and $\mathbf{u}_{sat}$ are the solutions of problem (3.2) which satisfy the iteration threshold as E_{tol} and $\widehat{E}_{tol}$, respectively.

(4) Using the same mesh as first-order auxiliary cell functions, the second-order auxiliary cell functions (2.38)-(2.50), which correspond to different macro-scale parameters (r_{s_1},T_{s_2}), are solved on $V_{h_1}(Y)$, respectively.

(5) For arbitrary point $(\mathbf{x},t)\in\Omega\times(0,T^*)$, we use the interpolation method to get the corresponding values of first-order auxiliary cell functions, second-order auxiliary cell functions and homogenized solutions. The spatial derivatives $\varepsilon_{mn}^{(0)*}$, $\psi_j(\varepsilon_{mn}^{(0)*})$, $\psi_m(T^{(0)})$ and $\psi_m\psi_n(T^{(0)})$ in Theorem 2.1 are evaluated by the average technique on relative elements [16, 17, 20, 21], and the temporal derivatives $\frac{\partial T^{(0)}}{\partial t}$, $\frac{\partial^2 u_i^{(0)}}{\partial t^2}$, $\frac{\partial \varepsilon_{mn}^{(0)*}}{\partial t}$ in Theorem 1 are evaluated by using the difference schemes (3.1) at every time steps. Then, the displacement field $\mathbf{u}^{(2\varepsilon)}(\mathbf{x},t)$ and temperature field $T^{(2\varepsilon)}(\mathbf{x},t)$ can be solved by the formulas (2.51) and (2.52). Moreover, we can still use the higher-order interpolation method and post-processing technique to get the high-precision SOTS solutions [22, 25].

4 Numerical examples and discussion

In this section, four numerical examples are given to verify the validity and feasibility of the SOTS numerical algorithm we developed. Since it is difficult to find the analytical solutions for the nonlinear two-way coupled system (2.1), we replace $T^\varepsilon(\mathbf{x},t)$ and $\mathbf{u}^\varepsilon(\mathbf{x},t)$ with $T_e(\mathbf{x},t)$ and $\mathbf{u}_e(\mathbf{x},t)$ which are precise FEM solutions for problem (2.1) on a very fine mesh. Without confusion, some notations are introduced as follows:

$$\mathbf{T}error0=\frac{||T_e-T^{(0)}||_{L^2}}{||T_e||_{L^2}},\ \mathbf{T}error1=\frac{||T_e-T^{(1\varepsilon)}||_{L^2}}{||T_e||_{L^2}},\ \mathbf{T}error2=\frac{||T_e-T^{(2\varepsilon)}||_{L^2}}{||T_e||_{L^2}}, \tag{4.1}$$

$$\mathbf{T}Error0=\frac{|T_e-T^{(0)}|_{H^1}}{|T_e|_{H^1}},\ \mathbf{T}Error1=\frac{|T_e-T^{(1\varepsilon)}|_{H^1}}{|T_e|_{H^1}},\ \mathbf{T}Error2=\frac{|T_e-T^{(2\varepsilon)}|_{H^1}}{|T_e|_{H^1}}, \tag{4.2}$$

$$\mathbf{u}error0=\frac{||\mathbf{u}_e-\mathbf{u}^{(0)}||_{L^2}}{||\mathbf{u}_e||_{L^2}},\ \mathbf{u}error1=\frac{||\mathbf{u}_e-\mathbf{u}^{(1\varepsilon)}||_{L^2}}{||\mathbf{u}_e||_{L^2}},\ \mathbf{u}error2=\frac{||\mathbf{u}_e-\mathbf{u}^{(2\varepsilon)}||_{L^2}}{||\mathbf{u}_e||_{L^2}}, \tag{4.3}$$

$$\mathbf{u}Error0=\frac{|\mathbf{u}_e-\mathbf{u}^{(0)}|_{H^1}}{|\mathbf{u}_e|_{H^1}},\ \mathbf{u}Error1=\frac{|\mathbf{u}_e-\mathbf{u}^{(1\varepsilon)}|_{H^1}}{\mathbf{u}_e|_{H^1}},\ \mathbf{u}Error2=\frac{|\mathbf{u}_e-\mathbf{u}^{(2\varepsilon)}|_{H^1}}{\mathbf{u}_e|_{H^1}}, \tag{4.4}$$

where $|\mathbf{u}_e-\mathbf{u}^{(0)}|_{H^1}=\left(\sum_{i,j=1}^n\left|\left|\varepsilon_{ij}(\mathbf{u}_e-\mathbf{u}^{(0)})\right|\right|_{L^2}\right)^{\frac{1}{2}}$.

https://doi.org/10.4208/cicp.OA-2016-0135 Published online by Cambridge University Press

4.1 Example 1: Plane stress problem with periodic structure in radial and hoop direction

In this example, a cylinder shell with fiber reinforced is considered. The material parameters of this example don't depend on temperature variable. The macrostructure Ω and unit cell Y are shown in Fig. 2, where $\Omega=(r,\theta)=[\pi,\frac{3}{2}\pi]\times[0,\pi]$ and periodic unit cell size $\varepsilon=\frac{\pi}{12}$.

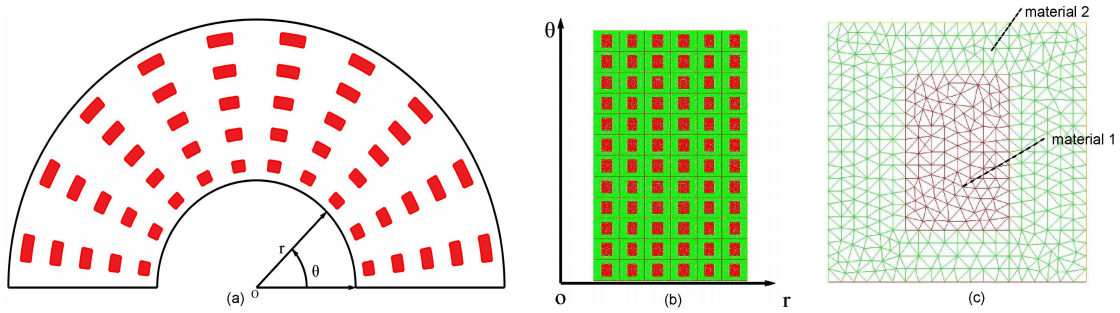


Figure 2: (a) Actual physical area; (b) Computational domain Ω; (c) Unit cell Y.

The non-dimensional material property parameters are listed in Table 1.

Table 1: Material property parameters.

Property	Matrix	Inclusion
Young's modulus	E=3.0×10^7	E=1.5×10^4
Poisson's ratio	ν=0.3	ν=0.25
Mass density	ρ=10.0	ρ=1.0
Specific heat	c=1.0	c=0.1
Thermal modulus	β_{ij}=50.0(i=j) or 0	β_{ij}=1.0(i=j) or 0
Thermal conductivity	k_{ij}=3.3(i=j) or 0	k_{ij}=0.01(i=j) or 0

The data in problem (2.1) are given as follows:

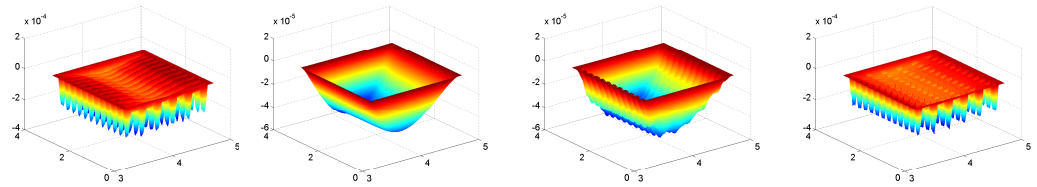
$$\begin{aligned}&f_1(\mathbf{x})=-2000,\ \ f_2(\mathbf{x})=-2000,\ \ h=200,\\&\widehat{\mathbf{u}}(\mathbf{x},t)=0,\ \ \widehat{T}(\mathbf{x},t)=20.0\ \text{ in }\partial\Omega,\\&\mathbf{u}^0(\mathbf{x})=0,\ \ \mathbf{u}^1(\mathbf{x})=0,\breve{T}(\mathbf{x})=20.0,\ \ \widetilde{T}=20.0\ \text{ in }\Omega.\end{aligned}\tag{4.5}$$

Now, the computational cost of FEM elements and nodes is listed in Table 2. After numerical calculation, Figs. 3-6 show the numerical results for solutions $u_1^\varepsilon,u_1^{(0)},u_1^{(1\varepsilon)},u_1^{(2\varepsilon)}$ and $u_2^\varepsilon,u_2^{(0)},u_2^{(1\varepsilon)},u_2^{(2\varepsilon)}$ and $T^\varepsilon,T^{(0)},T^{(1\varepsilon)},T^{(2\varepsilon)}$ and $\sigma_{11}^\varepsilon,\sigma_{11}^{(0)},\sigma_{11}^{(1\varepsilon)},\sigma_{11}^{(2\varepsilon)}$, respectively. Furthermore, the evolutive relative errors of displacement and temperature fields are shown in Fig. 7.

https://doi.org/10.4208/cicp.OA-2016-0135 Published online by Cambridge University Press

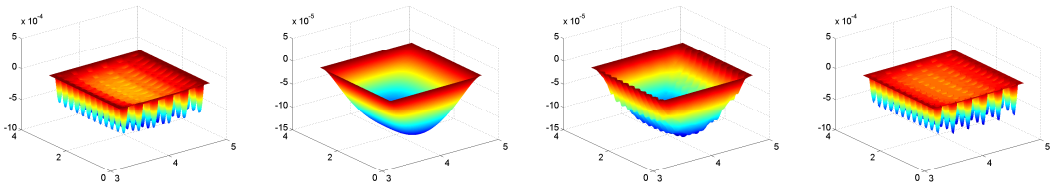
Table 2: Comparison of computational cost (Δt=0.002, $t\in$ [0,1]).

	Original equation	Cell problem	Homogenized equation
number of elements	48240	854	3600
number of nodes	24445	468	1891



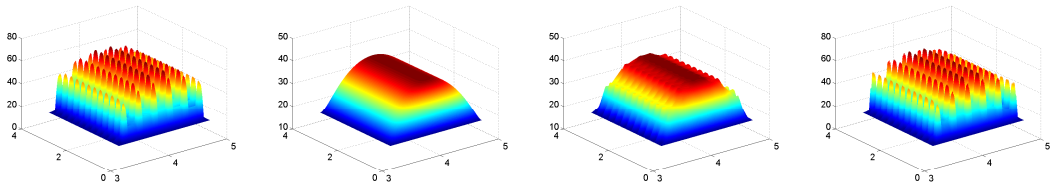
(a) (b) (c) (d)

Figure 3: The first component of the displacement field at time $t=1.0$: (a) u_1^ε; (b) $u_1^{(0)}$; (c) $u_1^{(1\varepsilon)}$; (d) $u_1^{(2\varepsilon)}$.



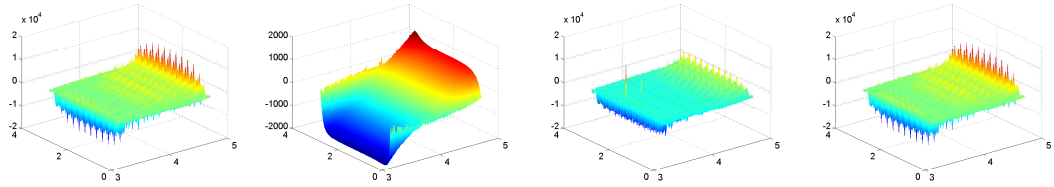
(a) (b) (c) (d)

Figure 4: The second component of the displacement field at time $t=1.0$: (a) u_2^ε; (b) $u_2^{(0)}$; (c) $u_2^{(1\varepsilon)}$; (d) $u_2^{(2\varepsilon)}$.



(a) (b) (c) (d)

Figure 5: The temperature field at time $t=1.0$: (a) T^ε; (b) $T^{(0)}$; (c) $T^{(1\varepsilon)}$; (d) $T^{(2\varepsilon)}$.



(a) (b) (c) (d)

Figure 6: The first component of the stress field at time $t=1.0$: (a) σ_{11}^ε; (b) $\sigma_{11}^{(0)}$; (c) $\sigma_{11}^{(1\varepsilon)}$; (d) $\sigma_{11}^{(2\varepsilon)}$.

https://doi.org/10.4208/cicp.OA-2016-0135 Published online by Cambridge University Press

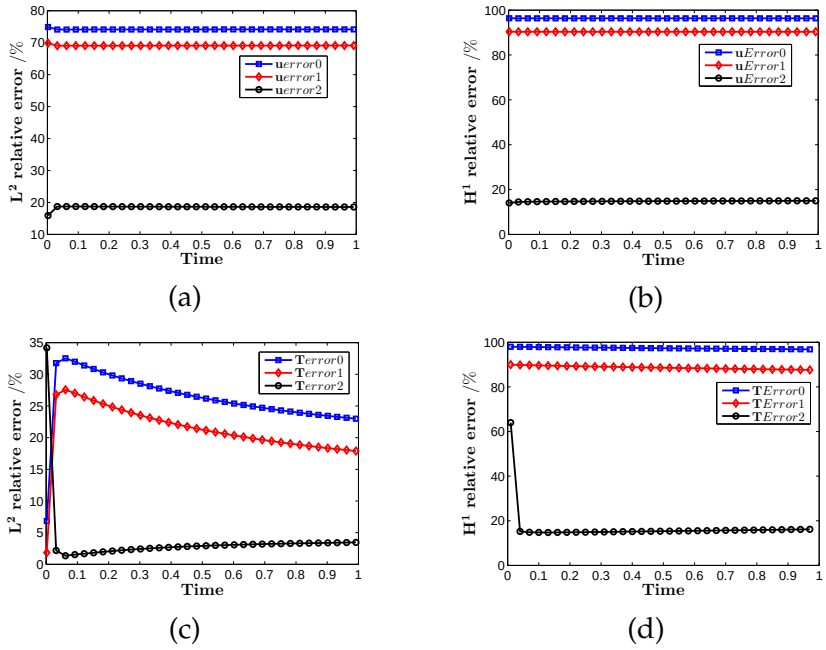


Figure 7: The evolutive relative errors of displacement and temperature fields: (a) $\mathbf{u}error$; (b) $\mathbf{u}Error$; (c) $Terror$; (d) $TError$.

From Table 2, one can see that the computational cost of SOTS method is much less than that of the precise FEM. It means that the SOTS method can greatly save computer memory, which is very important in engineering computation. Figs. 3-6 demonstrate that only SOTS solutions, which are almost the same as the precise FEM solutions, can accurately capture the micro-scale oscillating information due to heterogeneities in composites. By contrast, homogenized and FOTS solutions are far from enough to provide a high accuracy solution for multiscale problem (2.1). Besides, it is clear to see that the accuracy of SOTS solutions is much better than homogenized and FOTS solutions whether it is the relative error of temperature or displacement fields from Fig. 7. It means that the SOTS solutions is vital to capture micro-scale fluctuation information due to the heterogeneities of composite materials and our SOTS numerical algorithm is stable and effective after long-time numerical calculation.

4.2 Example 2: Axisymmetric problem with linear temperature-dependent material parameters

This example discussed axisymmetric problem with linear temperature-dependent material parameters, and periodic configurations in axial and radial direction of cylindrical coordinates. The macrostructure Ω and unit cell Y are shown in Fig. 8, where $\Omega=(r,z)=[1,1.5]\times[0,1]$ and periodic unit cell size $\varepsilon=\frac{1}{12}$. It is worth noting that the actual

https://doi.org/10.4208/cicp.OA-2016-0135 Published online by Cambridge University Press

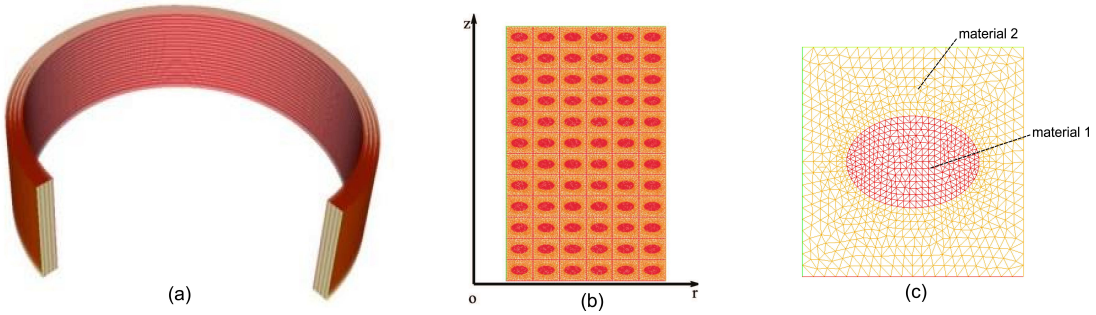


Figure 8: (a) Actual physical area (see [24]); (b) Computational domain Ω; (c) Unit cell Y.

physical area Fig. 8(a) is in accord with the computational domain Fig. 8(b) because there is no need to carry out the geometric transformation for the axisymmetric problem. The computational domain Ω of this axisymmetric problem is only a cross-section of actual physical area Fig. 8(a).

The non-dimensional material property parameters are listed in Table 3.

Table 3: Material property parameters (T represents temperature).

Property	Matrix	Inclusion
Young's modulus	E=3.0×10^7-5.0×10^3T	E=1.5×10^5-50.0T
Poisson's ratio	ν=0.3	ν=0.25
Mass density	ρ=45.0	ρ=4.5
Specific heat	c=1.2-0.002T	c=0.6-0.001T
Thermal modulus	β_{ij}=50.0-0.01T(i=j) or 0	β_{ij}=5.0-0.001T(i=j) or 0
Thermal conductivity	k_{ij}=15.0+5.0×10^{-3}T(i=j) or 0	k_{ij}=0.15+5.0×10^{-5}T(i=j) or 0

The data in problem (2.1) are given as follows:

$$\begin{aligned} &f_1(\mathbf{x})=-2000,\ f_3(\mathbf{x})=-2000,\ h=10000,\\ &\widehat{\mathbf{u}}(\mathbf{x},t)=0,\ \widehat{T}(\mathbf{x},t)=100.0\ \text{ in } \partial\Omega,\\ &\mathbf{u}^0(\mathbf{x})=0,\ \mathbf{u}^1(\mathbf{x})=0, \breve{T}(\mathbf{x})=100.0,\ \widetilde{T}=100.0\ \text{ in } \Omega. \end{aligned} \tag{4.6}$$

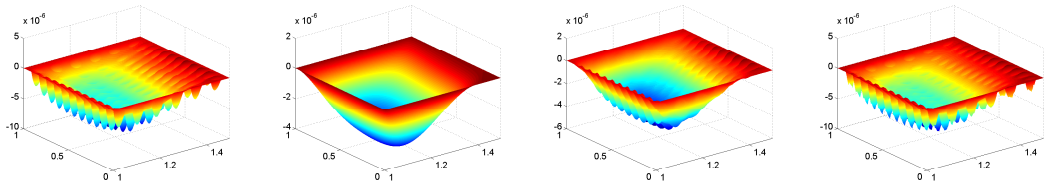
As Example 1, we list the computational cost of FEM elements and nodes in Table 4. After numerical calculation, Figs. 9-12 exhibit the numerical results for solutions u_1^ε,$u_1^{(0)}$,$u_1^{(1\varepsilon)}$,$u_1^{(2\varepsilon)}$ and u_3^ε,$u_3^{(0)}$,$u_3^{(1\varepsilon)}$,$u_3^{(2\varepsilon)}$ and T^ε,$T^{(0)}$,$T^{(1\varepsilon)}$,$T^{(2\varepsilon)}$ and σ_{11}^ε,$\sigma_{11}^{(0)}$,$\sigma_{11}^{(1\varepsilon)}$,$\sigma_{11}^{(2\varepsilon)}$, respectively. Furthermore, the evolutive relative errors of displacement and temperature fields are shown in Fig. 13.

From Table 4, one can easily see that the computational cost of SOTS method still is much less than that of the precise FEM. Moreover, from Figs. 9-12 we can find that only SOTS solutions agree reasonably well with the precise FEM solutions based on fine

https://doi.org/10.4208/cicp.OA-2016-0135 Published online by Cambridge University Press

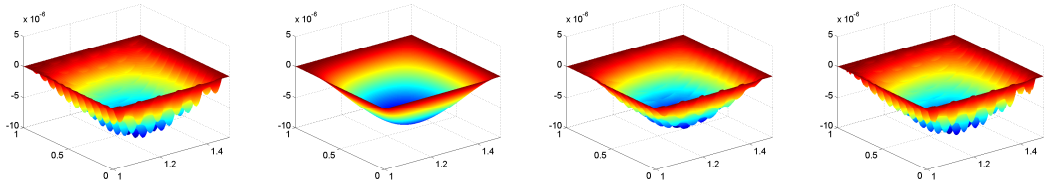
Table 4: Comparison of computational cost (Δt=0.002, $t\in$ [0,1]).

	Original equation	Cell problem	Homogenized equation
number of elements	49824	904	3600
number of nodes	25237	493	1891



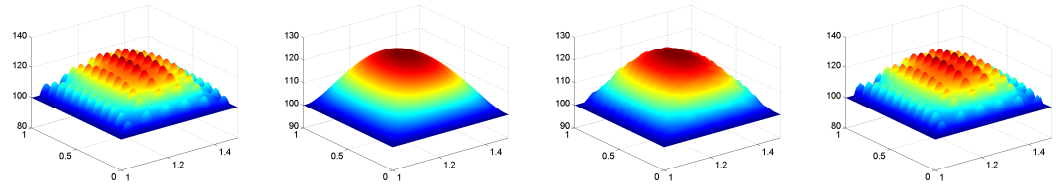
(a) (b) (c) (d)

Figure 9: The first component of the displacement field at time $t=1.0$: (a) u_1^ε; (b) $u_1^{(0)}$; (c) $u_1^{(1\varepsilon)}$; (d) $u_1^{(2\varepsilon)}$.



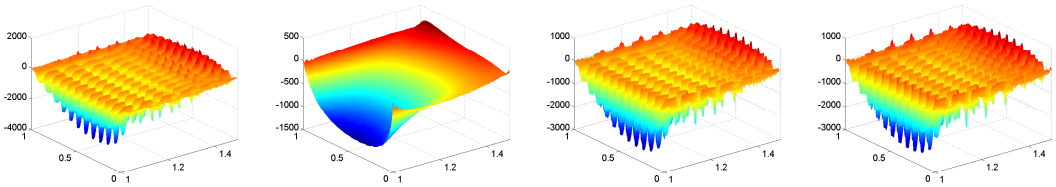
(a) (b) (c) (d)

Figure 10: The third component of the displacement field at time $t=1.0$: (a) u_3^ε; (b) $u_3^{(0)}$; (c) $u_3^{(1\varepsilon)}$; (d) $u_3^{(2\varepsilon)}$.



(a) (b) (c) (d)

Figure 11: The temperature field at time $t=1.0$: (a) T^ε; (b) $T^{(0)}$; (c) $T^{(1\varepsilon)}$; (d) $T^{(2\varepsilon)}$.



(a) (b) (c) (d)

Figure 12: The first component of the stress field at time $t=1.0$: (a) σ_{11}^ε; (b) $\sigma_{11}^{(0)}$; (c) $\sigma_{11}^{(1\varepsilon)}$; (d) $\sigma_{11}^{(2\varepsilon)}$.

https://doi.org/10.4208/cicp.OA-2016-0135 Published online by Cambridge University Press

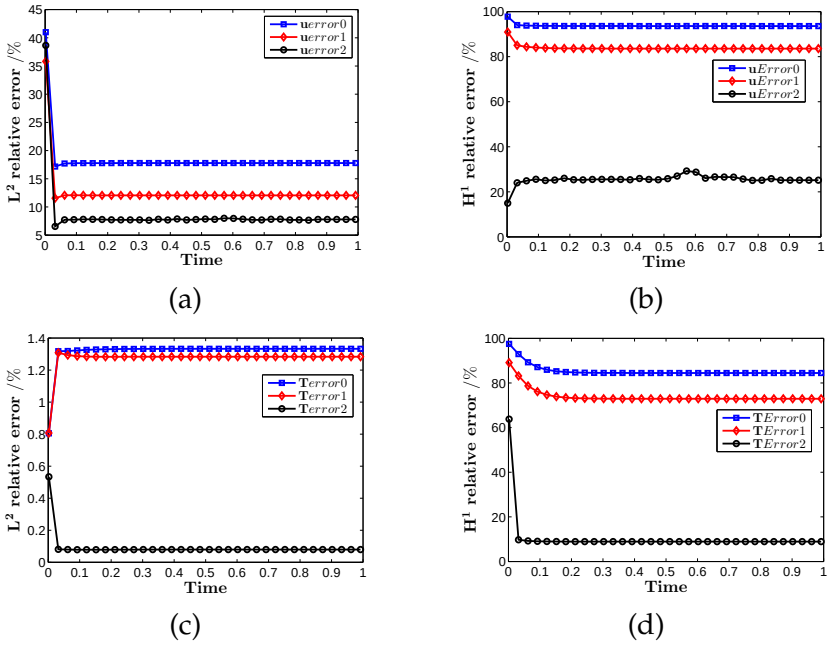


Figure 13: The evolutive relative errors of displacement and temperature fields: (a) $\mathbf{u}error$; (b) $\mathbf{u}Error$; (c) $Terror$; (d) $TError$.

meshes, and the homogenized and FOTS solutions can't capture the micro-scale oscillation of the displacement and temperature fields. From Fig. 13, it is easy to find that only the SOTS solutions can provide enough numerical accuracy for engineering applications. The accuracy of homogenized solutions and FOTS solutions is far from enough especially in the H^1 semi-norm sense.

4.3 Example 3: Axisymmetric problem with quadratic temperature-dependent material parameters

The axisymmetric problem with quadratic temperature-dependent material parameters, and periodic structure in axial and radial direction of cylindrical coordinates is investigated in this example. The macrostructure Ω and unit cell Y of this example are identical to Example 2, where $\Omega=(r,z)=[1,1.5]\times[0,1]$ but periodic unit cell size $\varepsilon=\frac{1}{24}$ which means that this example has a large number of inclusions than Example 2. The non-dimensional material property parameters are listed in Table 5.

The data in problem (2.1) are given as follows:

$$\begin{aligned}&f_1(\mathbf{x})=-2000,\ \ f_2(\mathbf{x})=-2000,\ \ h=10000,\\&\widehat{\mathbf{u}}(\mathbf{x},t)=0,\ \ \widehat{T}(\mathbf{x},t)=200.0\ \text{ in }\partial\Omega,\\&\mathbf{u}^0(\mathbf{x})=0,\ \ \mathbf{u}^1(\mathbf{x})=0,\check{T}(\mathbf{x})=200.0,\ \ \widetilde{T}=200.0\ \text{ in }\Omega.\end{aligned}\tag{4.7}$$

https://doi.org/10.4208/cicp.OA-2016-0135 Published online by Cambridge University Press

Table 5: Material property parameters (T represents temperature).

Property	Matrix	Inclusion
Young's modulus	E=3.0×10^7-5.0×10^3T-3.0×10$^{-2}T^2$	E=1.5×10^5-50.0T-1.5×10$^{-4}T^2$
Poisson's ratio	ν=0.3	ν=0.25
Mass density	ρ=45.0	ρ=4.5
Specific heat	c=1.2-0.002T-0.00002T^2	c=0.6-0.001T-0.00001T^2
Thermal modulus	β_{ij}=50.0-0.01T-0.001T^2(i=j) or 0	β_{ij}=5.0-0.001T-0.00001T^2(i=j) or 0
Thermal conductivity	k_{ij}=15.0+5.0×10^{-3}T+2.5×10$^{-5}T^2$ (i=j) or 0	k_{ij}=0.15+5.0×10^{-5}T+2.5×10$^{-7}T^2$ (i=j) or 0

In Table 6, the computational cost of precious FEM and SOTS method is listed in detail. We can find that the computational cost of SOTS method is much less than that of the precise FEM.

Table 6: Comparison of computational cost (Δt=0.002, $t\in$ [0,1]).

	Original equation	Cell problem	Homogenized equation
number of elements	199296	904	3600
number of nodes	100297	493	1891

After numerical computation, some final numerical results are exhibited in Figs. 14-18. Figs. 14-17 show the numerical results for solutions u_1^ε,$u_1^{(0)}$,$u_1^{(1\varepsilon)}$,$u_1^{(2\varepsilon)}$ and u_3^ε,$u_3^{(0)}$,$u_3^{(1\varepsilon)}$,$u_3^{(2\varepsilon)}$ and T^ε,$T^{(0)}$,$T^{(1\varepsilon)}$,$T^{(2\varepsilon)}$ and σ_{11}^ε,$\sigma_{11}^{(0)}$,$\sigma_{11}^{(1\varepsilon)}$,$\sigma_{11}^{(2\varepsilon)}$, respectively. The evolutive relative errors of displacement and temperature fields are shown in Fig. 18.

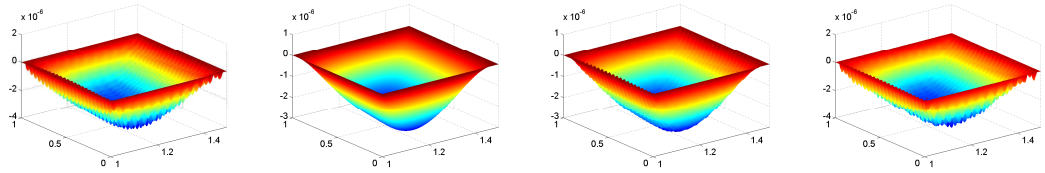
In summary, it can be seen from Figs. 14-17 that homogenized and FOTS solutions can't precisely capture the micro-scale oscillating behavior and only SOTS solutions are in good agreement with the precise FEM solutions. From Fig. 18, it is clear to see that only SOTS solutions can provide enough numerical accuracy not only in L^2 norm but also in H^1 semi-norm. Moreover, the high accuracy of SOTS solutions in H^1 semi-norm sense means that SOTS solutions can provide high precision solutions of the heat flux and strains for practical engineering applications.

4.4 Example 4: The analysis of nonlinear two-way coupled response

In this example, we analyze the nonlinear two-way coupled response of multiscale problem (2.1). The axisymmetric problems with temperature-independent, linear and quadratic temperature-dependent material parameters will be discussed and compared in this example. The specific patterns of material parameters are listed in Table 7.

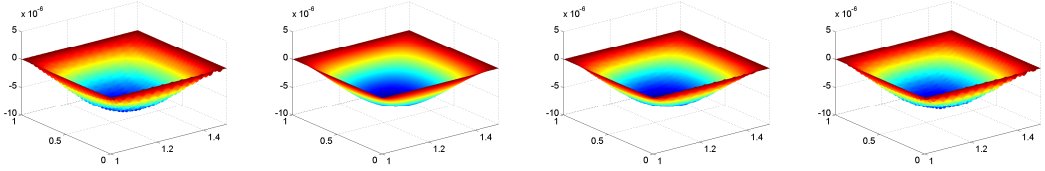
The macrostructure Ω and unit cell Y of this example are identical to Example 2. The non-dimensional quadratic temperature-dependent material parameters of this example

https://doi.org/10.4208/cicp.OA-2016-0135 Published online by Cambridge University Press



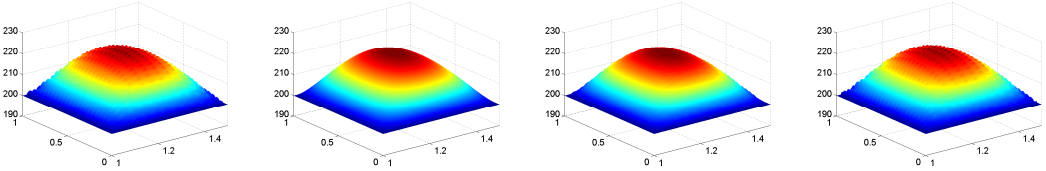
(a) (b) (c) (d)

Figure 14: The first component of the displacement field at time $t=1.0$: (a) u_1^{ε}; (b) $u_1^{(0)}$; (c) $u_1^{(1\varepsilon)}$; (d) $u_1^{(2\varepsilon)}$.



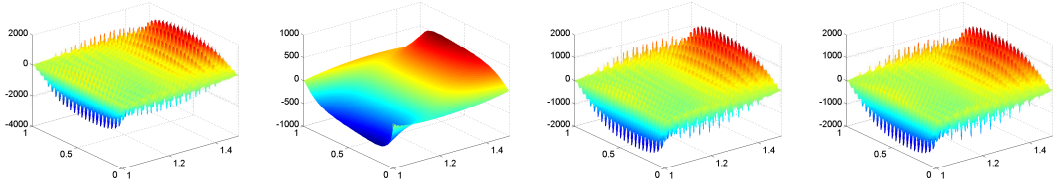
(a) (b) (c) (d)

Figure 15: The third component of the displacement field at time $t=1.0$: (a) u_3^{ε}; (b) $u_3^{(0)}$; (c) $u_3^{(1\varepsilon)}$; (d) $u_3^{(2\varepsilon)}$.



(a) (b) (c) (d)

Figure 16: The temperature field at time $t=1.0$: (a) T^{ε}; (b) $T^{(0)}$; (c) $T^{(1\varepsilon)}$; (d) $T^{(2\varepsilon)}$.



(a) (b) (c) (d)

Figure 17: The first component of the stress field at time $t=1.0$: (a) $\sigma_{11}^{\varepsilon}$; (b) $\sigma_{11}^{(0)}$; (c) $\sigma_{11}^{(1\varepsilon)}$; (d) $\sigma_{11}^{(2\varepsilon)}$.

https://doi.org/10.4208/cicp.OA-2016-0135 Published online by Cambridge University Press

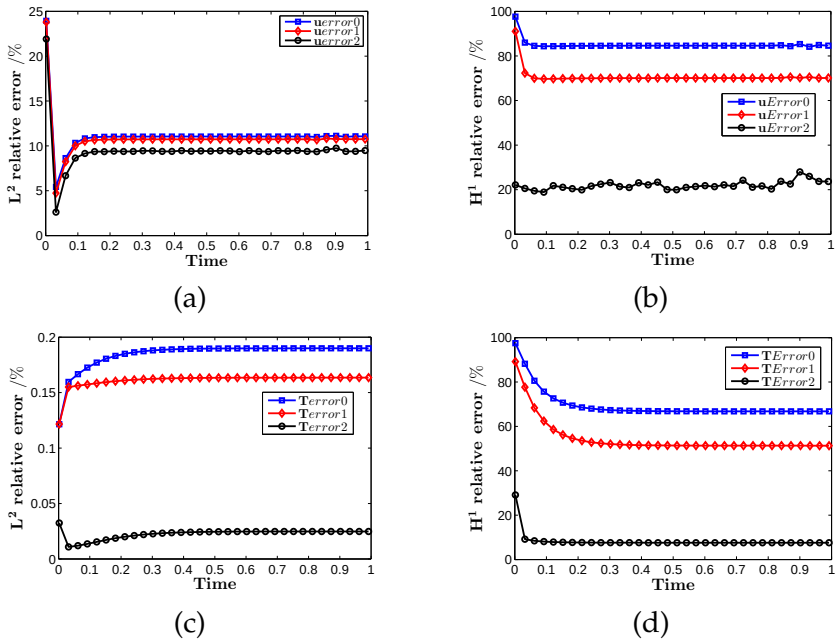


Figure 18: The evolutive relative errors of displacement and temperature fields: (a) $\mathbf{u}error$; (b) $\mathbf{u}Error$; (c) $Terror$; (d) $TError$.

Table 7: Material property parameters (T represents temperature).

material property	specific pattern
temperature-independent	a
linear temperature-dependent	$a+bT$
quadratic temperature-dependent	$a+bT+cT^2$

are the same as Example 3. The data in problem (2.1) are given as follows:

$$\begin{aligned} &f_1(\mathbf{x})=-1500,\ \ f_3(\mathbf{x})=-1500,\ \ h=9000,\\ &\widehat{\mathbf{u}}(\mathbf{x},t)=0,\ \ \widehat{T}(\mathbf{x},t)=400.0\ \text{ in }\partial\Omega,\\ &\mathbf{u}^0(\mathbf{x})=0,\ \ \mathbf{u}^1(\mathbf{x})=0,\ \ \breve{T}(\mathbf{x})=400.0,\ \ \widetilde{T}=400.0;\ \text{ in }\Omega. \end{aligned} \tag{4.8}$$

After numerical computation, we depict the final numerical results in Fig. 19.

From Fig. 19, it can be easily seen that the final SOTS solutions for multiscale problem (2.1) with three different kinds of material parameters are quite different, especially between temperature-independent and quadratic temperature-dependent material parameters. In conclusion, the temperature-dependent properties of the composites should be taken into account when the composites serve in high-temperature circumstances. Only by this way, we can obtain more accurate analyses of the composites' thermo-mechanical behavior.

https://doi.org/10.4208/cicp.OA-2016-0135 Published online by Cambridge University Press

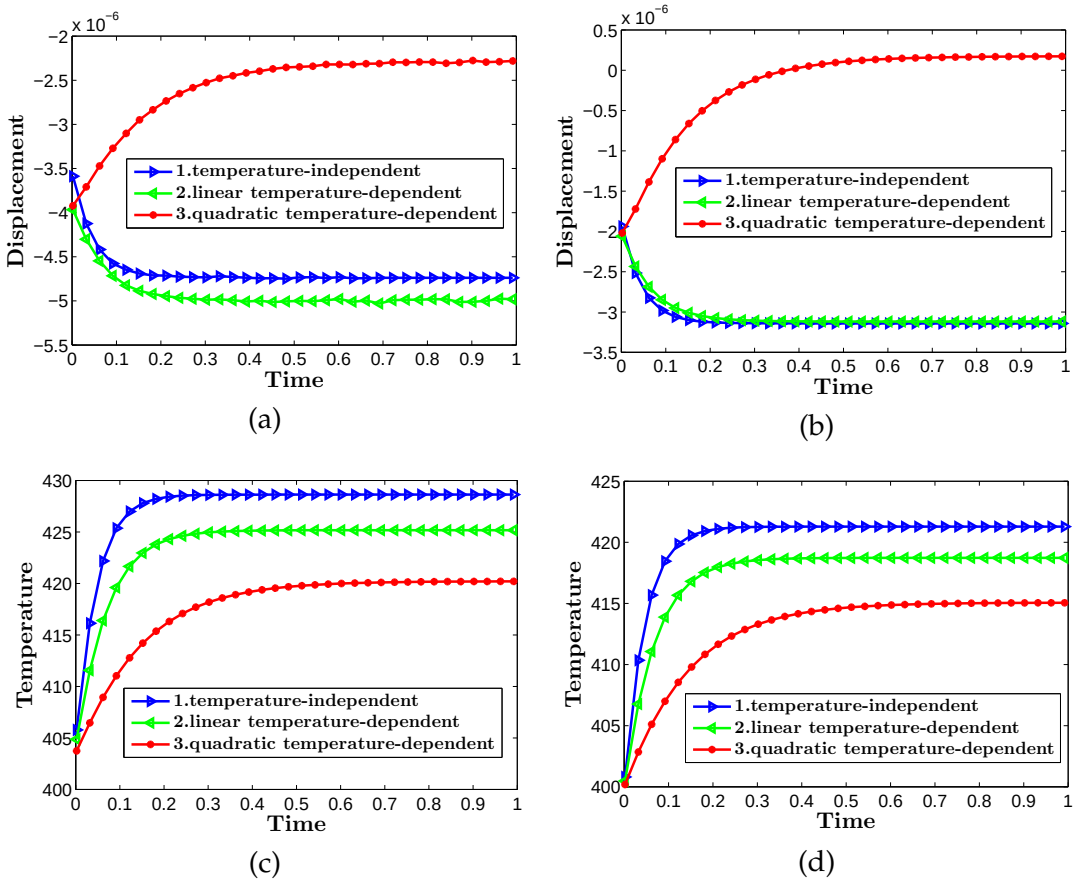


Figure 19: The displacement and temperature fields of different fixed points: (a) $u_1^{(2\varepsilon)}$ in Inclusion point (1.2083,0.4583); (b) $u_1^{(2\varepsilon)}$ in Matrix point (1.1667,0.4167); (c)$T^{(2\varepsilon)}$ in Inclusion point (1.2083,0.4583); (d)$T^{(2\varepsilon)}$ in Matrix point (1.1667,0.4167).

5 Conclusions

In this paper, we develop a SOTS computational method for nonlinear dynamic thermo-mechanical problems of composites with cylindrical periodicity. The new contributions of this paper are the determination of the SOTS solutions, the error analysis in the point-wise sense and the presentation of a SOTS numerical algorithm. Numerical experiments show that the SOTS numerical method we proposed is stable and effective for multi-scale problem (2.1), and can greatly save computer memory. It is essentially stressed that in most cases the direct FEM solving for multiscale problem (2.1) is unstable and non-convergent. Furthermore, numerical results show that only SOTS solutions can accurately capture the micro-scale oscillating information and provide enough numerical accuracy for engineering applications.

https://doi.org/10.4208/cicp.OA-2016-0135 Published online by Cambridge University Press

Acknowledgments

This research was supported by the National Natural Science Foundation of China (No. 11501449 and No. 11471262), the National Basic Research Program of China (No. 2012CB025904), and also supported by the Center for high performance computing of Northwestern Polytechnical University.

Appendix A

In this section, we will show the detailed forms of $S_{0i}(\mathbf{x},\mathbf{y},t)$, $S_{1i}(\mathbf{x},\mathbf{y},t)$, $F_0(\mathbf{x},\mathbf{y},t)$, $F_1(\mathbf{x},\mathbf{y},t)$, $H_i(\mathbf{x},\mathbf{y},t)$ and $G(\mathbf{x},\mathbf{y},t)$ in Subsection 2.2:

$$\begin{aligned}S_{0i}(\mathbf{x},\mathbf{y},t)=&(\widehat{\rho}-\rho^{(0)})\frac{\partial^2 u_i^{(0)}}{\partial t^2}+\psi_j\Big[\big(\widehat{C}_{ijkl}-C_{ijkl}^{(0)}-C_{ijmn}^{(0)}\widetilde{\psi}_m(N_n^{kl})\big)\cdot\varepsilon_{kl}^{(0)*}\Big]\\&+\widetilde{\psi}_j\big[C_{ijmn}^{(0)}\widetilde{\psi}_m(N_n^{kl}\varepsilon_{kl}^{(0)*})\big]+\psi_j\big[\beta_{ij}^{(0)}T^{(0)}+C_{ijkl}^{(0)}\widetilde{\psi}_k(P_l)T^{(0)}-\widehat{\beta}_{ij}T^{(0)}\big]\\&+\psi_j\big[\widetilde{\psi}_k(C_{ikjl}^{(0)}P_l)T^{(0)}+\widetilde{\psi}_k(\beta_{ik}^{(0)}M^j)T^{(0)}\big]+\delta_{i1}\frac{V_{11}-V_{22}}{r}+\delta_{i2}\frac{2V_{12}}{r}+\delta_{i3}\frac{V_{31}}{r},\end{aligned}\tag{A.1}$$

where the operators $V_{ij}=C_{ijkl}^{(0)}\widetilde{\psi}_k(N_l^{mn})\varepsilon_{mn}^{(0)*}-C_{ijkl}^{(0)}\widetilde{\psi}_k(P_l)(T^{(0)}-\widetilde{T})$;

$$\begin{aligned}S_{1i}(\mathbf{x},\mathbf{y},t)=&-\rho^{(0)}N_i^{kl}\frac{\partial^2\varepsilon_{kl}^{(0)*}}{\partial t^2}+\rho^{(0)}P_i\frac{\partial^2 T^{(0)}}{\partial t^2}+\psi_j\big[C_{ijkl}^{(0)}\varepsilon_{kl}^{(0)*}(\mathbf{N}^{mn}\varepsilon_{mn}^{(0)*})\big]\\&-\psi_j\Big[C_{ijkl}^{(0)}\varepsilon_{kl}^{(0)*}\big(\mathbf{P}(T^{(0)}-\widetilde{T})\big)\Big]-\psi_j\big[\beta_{ij}^{(0)}M^m\psi_m(T^{(0)})\big]\\&+\delta_{i1}\frac{W_{11}-W_{22}}{r}+\delta_{i2}\frac{2W_{12}}{r}+\delta_{i3}\frac{W_{31}}{r},\end{aligned}\tag{A.2}$$

where the operators $W_{ij}=C_{ijkl}^{(1)}\widetilde{\psi}_k(N_l^{mn})\varepsilon_{mn}^{(0)*}-C_{ijkl}^{(1)}\widetilde{\psi}_k(P_l)(T^{(0)}-\widetilde{T})+C_{ijkl}^{(0)}\varepsilon_{kl}^{(0)*}(\mathbf{N}^{mn}\varepsilon_{mn}^{(0)*})-C_{ijkl}^{(0)}\varepsilon_{kl}^{(0)*}(\mathbf{P}(T^{(0)}-\widetilde{T})$;

$$\begin{aligned}F_0(\mathbf{x},\mathbf{y},t)=&\big[\widehat{S}-\rho^{(0)}c^{(0)}+\vartheta_{ij}\psi_i(P_j)\big]\frac{\partial T^{(0)}}{\partial t}+\psi_i\Big[\big(k_{ij}^{(0)}-\widehat{k}_{ij}+k_{im}^{(0)}\widetilde{\psi}_m(M^j)\big)\cdot\psi_j(T^{(0)})\Big]\\&+\widetilde{\psi}_i\big[k_{im}^{(0)}\psi_m(M^m\psi_j(T^{(0)}))\big]+\frac{\big[k_{1j}^{(0)}-\widehat{k}_{1j}+k_{1m}^{(0)}\widetilde{\psi}_m(M^j)\big]\psi_j(T^{(0)})}{r}\\&+\big[\vartheta_{ij}^{(0)}-\widehat{\vartheta}_{ij}+\vartheta_{mn}^{(0)}\widetilde{\psi}_m(N_n^{ij})\big]\frac{\partial\varepsilon_{ij}^{(0)*}}{\partial t},\end{aligned}\tag{A.3}$$

$$\begin{aligned}F_1(\mathbf{x},\mathbf{y},t)=&-\rho^{(0)}c^{(0)}M^j\frac{\partial\psi_j(T^{(0)})}{\partial t}+\psi_i\big[k_{im}^{(0)}\psi_m(M^j\psi_j(T^{(0)}))\big]+\frac{k_{1m}^{(0)}\psi_m\big[M^j\psi_j(T^{(0)})\big]}{r}\\&-\vartheta_{ij}^{(0)}\frac{\partial}{\partial t}\Big[\varepsilon_{ij}^{(0)*}\big(\mathbf{N}^{mn}\varepsilon_{mn}^{(0)*}\big)\Big]+\vartheta_{ij}^{(0)}\frac{\partial}{\partial t}\Big[\varepsilon_{ij}^{(0)*}\big(\mathbf{P}(T^{(0)}-\widetilde{T})\big)\Big],\end{aligned}\tag{A.4}$$

https://doi.org/10.4208/cicp.OA-2016-0135 Published online by Cambridge University Press

$$
\begin{aligned}
H_i(\mathbf{x},\mathbf{y},t) = &-\rho^{(0)} N_i^{kl} \frac{\partial^2 \varepsilon_{kl}^{(0)*}}{\partial t^2} + \rho^{(0)} P_i \frac{\partial^2 T^{(0)}}{\partial t^2} + \psi_j \left[C_{ijkl}^{(0)} \varepsilon_{kl}^{(0)*} (\mathbf{N}^{mn} \varepsilon_{mn}^{(0)*}) \right] \\
&- \psi_j \left[C_{ijkl}^{(0)} \varepsilon_{kl}^{(0)*} \left(\mathbf{P}(T^{(0)} - \widetilde{T}) \right) \right] - \psi_j \left[\beta_{ij}^{(0)} M^m \psi_m (T^{(0)}) \right] \\
&+ \delta_{i1} \frac{W_{11} - W_{22}}{r} + \delta_{i2} \frac{2W_{12}}{r} + \delta_{i3} \frac{W_{31}}{r} + \psi_j \left[C_{ijkl}^{(0)} \widetilde{\psi}_k (u_l^{(2)}) \right] \\
&+ \widetilde{\psi}_j \left[C_{ijkl}^{(0)} \varepsilon_{kl}^{(0)*} (\mathbf{u}^{(2)}) \right] - \beta_{ij}^{(0)} T^{(2)} - \varepsilon \rho^{(0)} \frac{\partial^2 u_i^{(2)}}{\partial t^2} - \varepsilon \beta_{ij}^{(0)} T^{(2)} \\
&+ \varepsilon \psi_j \left[C_{ijkl}^{(0)} \varepsilon_{kl}^{(0)*} (\mathbf{u}^{(2)}) \right] + \varepsilon \delta_{i1} \frac{\eta_{11} - \eta_{22}}{r} + \varepsilon \delta_{i2} \frac{2\eta_{12}}{r} + \varepsilon \delta_{i3} \frac{\eta_{31}}{r}, \qquad \text{(A.5)}
\end{aligned}
$$

where the operators $\eta_{ij} = C_{ijkl}^{(0)} \widetilde{\psi}_k (u_l^{(2)}) + \varepsilon C_{ijkl}^{(0)} \varepsilon_{kl}^{(0)*} (\mathbf{u}^{(2)}) - \varepsilon \beta_{ij}^{(0)} T^{(2)}$;

$$
\begin{aligned}
G(\mathbf{x},\mathbf{y},t) = &-\rho^{(0)} c^{(0)} M^j \frac{\partial \psi_j (T^{(0)})}{\partial t} + \psi_i \left[k_{im}^{(0)} \psi_m (M^j \psi_j (T^{(0)})) \right] + \frac{k_{1m}^{(0)} \psi_m \left[M^j \psi_j (T^{(0)}) \right]}{r} \\
&- \vartheta_{ij}^{(0)} \frac{\partial}{\partial t} \left[\varepsilon_{ij}^{(0)*} \left(\mathbf{N}^{mn} \varepsilon_{mn}^{(0)*} \right) \right] + \vartheta_{ij}^{(0)} \frac{\partial}{\partial t} \left[\varepsilon_{ij}^{(0)*} \left(\mathbf{P}(T^{(0)} - \widetilde{T}) \right) \right] + \psi_i \left[k_{ij}^{(0)} \widetilde{\psi}_j (T^{(2)}) \right] \\
&+ \widetilde{\psi}_i \left[k_{ij}^{(0)} \widetilde{\psi}_j (T^{(2)}) \right] + \frac{k_{1j}^{(0)} \widetilde{\psi}_j (T^{(2)})}{r} + \vartheta_{ij}^{(0)} \frac{\partial}{\partial t} \left[\widetilde{\psi}_j (u_j^{(2)}) \right] - \varepsilon \rho^{(0)} c^{(0)} \frac{\partial T^{(2)}}{\partial t} \\
&+ \varepsilon \widetilde{\psi}_i \left[k_{ij}^{(0)} \psi_j (T^{(2)}) \right] + \varepsilon \frac{k_{1j}^{(0)} \psi_j (T^{(2)})}{r} + \varepsilon \vartheta_{ij}^{(0)} \frac{\partial \varepsilon_{ij}^{(0)*} (\mathbf{u}^{(2)})}{\partial t}. \qquad \text{(A.6)}
\end{aligned}
$$

References

[1] T. Matsumoto, A. Guzik, M. Tanaka, A boundary element method for analysis of thermoelastic deformations in materials with temperature dependent properties, International Journal for Numerical Methods in Engineering, 64 (2005), 1432-1458.

[2] H. W. Zhang, D. S. Yang, S. Zhang, Y. G. Zheng, Multiscale nonlinear thermoelastic analysis of heterogeneous multiphase materials with temperature-dependent properties, Finite Elements in Analysis and Design, 88 (2014), 97-117.

[3] J. N. Reddy, C. D. Chin, Thermomechanical analysis of functionally graded cylinders and plates, Journal of Thermal Stresses, 21 (1998), 593-626.

[4] M. R. E. Nasution, N. Watanabe, A. Kondo, A. Yudhanto, Thermo-mechanical properties and stress analysis of 3-d textile composites by asymptotic expansion homogenization method, Composites Part B-Engineering, 60 (2014), 378-391.

[5] Z. Q. Yang, J. Z. Cui, Y. Sun, J. R. Ge, Multiscale computation for transient heat conduction problem with radiation boundary condition in porous materials, Finite Elements in Analysis and Design, 102-103 (2015), 7-18.

[6] R. B. Hetnarski, M. R. Eslami, Thermal Stresses: Advanced Theory and Applications, Springer Verlag, Berlin, 2008.

[7] L. H. Wu, Z. Q. Jiang, J. Liu, Thermoelastic stability of functionally graded cylindrical shells, Composite Structures, 70 (2005), 60-68.

https://doi.org/10.4208/cicp.OA-2016-0135 Published online by Cambridge University Press

[8] G. Chatzigeorgiou, N. Charalambakis, F. Murat, Homogenization problems of a hollow cylinder made of elastic materials with discontinuous properties, International Journal of Solids and Structures, 45 (2008), 5165-5180.
[9] N. Charalambakis, G. Chatzigeorgiou, Y. Efendiev, D. Lagoudas, Effective behavior of composite structures made of thermoelastic constituents with cylindrical periodicity, volume 10 of Procedia Engineering, 2011, pp. 3602-3607.
[10] G. Chatzigeorgiou, Y. Efendiev, N. Charalambakis, D. C. Lagoudas, Effective thermoelastic properties of composites with periodicity in cylindrical coordinates, International Journal of Solids and Structures, 49 (2012), 2590-2603.
[11] J. J. Wan, Multi-scale Analysis Method for Dynamic Coupled Thermoelasticity of Composite Structures, Ph.D. thesis, Academy of Mathematics and Systems Sciences, Chinese Academy of Sciences, 2007.
[12] Z. H. Yang, J. Z. Cui, Y. T. Wu, Z. Q. Wang, J. J. Wan, Second-order two-scale analysis method for dynamic thermo-mechanical problems in periodic structure, International Journal of Numerical Analysis and Modeling, 12 (2015), 144-161.
[13] Z. Q. Yang, J. Z. Cui, Y. Sun, J. Liang, Z. H. Yang, Multiscale analysis method for thermo-mechanical performance of periodic porous materials with interior surface radiation, International Journal for Numerical Methods in Engineering, 105 (2016), 323-350.
[14] X. Wang, L. Q. Cao, Y. S. Wong, Multiscale computation and convergence for coupled thermoelastic system in composite materials, Multiscale Modeling & Simulation, 13 (2015), 661-690.
[15] J. Nečas, I. Hlaváček, Mathematical Theory of Elastic and Elasto-Plastic Bodies: An Introduction, Elsevier Academic Press, New York, 1981.
[16] Z. Q. Yang, J. Z. Cui, S. Zhou, Thermo-mechanical analysis of periodic porous materials with microscale heat transfer by multiscale asymptotic expansion method, International Journal of Heat and Mass Transfer, 92 (2016), 904-919.
[17] Q. Ma, J. Z. Cui, Second-order two-scale analysis method for the heat conductive problem with radiation boundary condition in periodical porous domain, Communications in Computational Physics, 14 (2013), 1027-1057.
[18] D. Cioranescu, P. Donato, An Introduction to Homogenization 1nd ed., Oxford University Press, London, 1999.
[19] Philippe G. Ciarlet, Mathematical Elasticity Volume III: Theory of Shells 1nd ed., North-Holland Publishing Company, Amsterdam, 2000.
[20] J. Z. Cui, Multiscale computational method for unified design of structure, components and their materials, in: Proceedings on Computational Mechanics in Science and Engineering, CCCM-2001, Guangzhou, 5-8 December, Peking University Press, 2001, pp. 33-43.
[21] L. Q. Cao, Multiscale asymptotic expansion and finite element methods for the mixed boundary value problems of second order elliptic equation in perforated domains, Numerische Mathematik, 103 (2006), 11-45.
[22] Q. L. Dong, L. Q. Cao, Multiscale asymptotic expansions methods and numerical algorithms for the wave equations in perforated domains, Applied Mathematics and Computation, 232 (2014), 872-887.
[23] Q. F. Zhang, J. Z. Cui, Existence theory for rosseland equation and its homogenized equation, Applied Mathematics and Mechanics-English Edition, 33 (2012), 1595-1612.
[24] Q. Ma, J. Z. Cui, Z. H. Li, Second-order two-scale asymptotic analysis for axisymmetric and spherical symmetric structure with periodic configurations, International Journal of Solids and Structures, 78-79 (2016), 77-100.

https://doi.org/10.4208/cicp.OA-2016-0135 Published online by Cambridge University Press

[25] Q. Lin, Q. D. Zhu, The Preprocessing and Postprocessing for the Finite Element Method, Shanghai Scientific & Technical Publishers, Shanghai, 1994.
[26] N. D. Duc, T. Q. Quan, Transient responses of functionally graded double curved shallow shells with temperature-dependent material properties in thermal environment, European Journal of Mechanics a-Solids, 47 (2014), 101-123.
[27] Y. Z. Wang, D. Liu, Q. Wang, C. Shu, Thermoelastic response of thin plate with variable material properties under transient thermal shock, International Journal of Mechanical Sciences, 104 (2015), 200-206.
[28] R. Kolahchi, M. Safari, M. Esmailpour, Dynamic stability analysis of temperature-dependent functionally graded cnt-reinforced visco-plates resting on orthotropic elastomeric medium, Composite Structures, 150 (2016), 255-265.
[29] Y. T. Wu, Y. F. Nie, Z. H. Yang, Comparison of four multiscale methods for elliptic problems, Cmes-Computer Modeling in Engineering & Sciences, 99 (2014), 297-325.
[30] M. Mierzwiczak, W. Chen, Z. J. Fu, The singular boundary method for steady-state nonlinear heat conduction problem with temperature-dependent thermal conductivity, International Journal of Heat and Mass Transfer, 91 (2015), 205-217.
[31] G. Chatzigeorgiou, N. Charalambakis, Y. Chemisky, F. Meraghni, Periodic homogenization for fully coupled thermomechanical modeling of dissipative generalized standard materials, International Journal of Plasticity, 81 (2016), 18-39.
[32] F. Han, J. Z. Cui, Y. F. Nie, The two-order and two-scale method in cylindrical coordinates for mechanical properties of laminated composite cylindrical structure. 8th. World Congress on Computational Mechanics (WCCM8) & 5th. European Congress on Computational Methods in Applied Sciences and Engineering (ECCOMAS 2008), 2008, Venice, Italy.
[33] F. Han, J. Z. Cui, Y. Yu, The statistical second-order two-scale method for thermomechanical properties of statistically inhomogeneous materials, Computational Materials Science, 46 (2009), 654-659.
[34] Y. Yu, J. Z. Cui, F. Han, The statistical second-order two-scale analysis method for heat conduction performances of the composite structure with inconsistent random distribution, Computational Materials Science, 46 (2009), 151-161.

https://doi.org/10.4208/cicp.OA-2016-0135 Published online by Cambridge University Press